ERDC/EL TR-23-4

US Army Corps of Engineers®
Engineer Research and Development Center

ERDC
ENGINEER RESEARCH & DEVELOPMENT CENTER

Dredging Operations and Environmental Research (DOER) Program

Improving Spatial and Temporal Monitoring of Dredging Operations Incorporating Unmanned Technologies

Justin L. Wilkens, Andrew D. McQueen, and Burton C. Suedel

August 2023

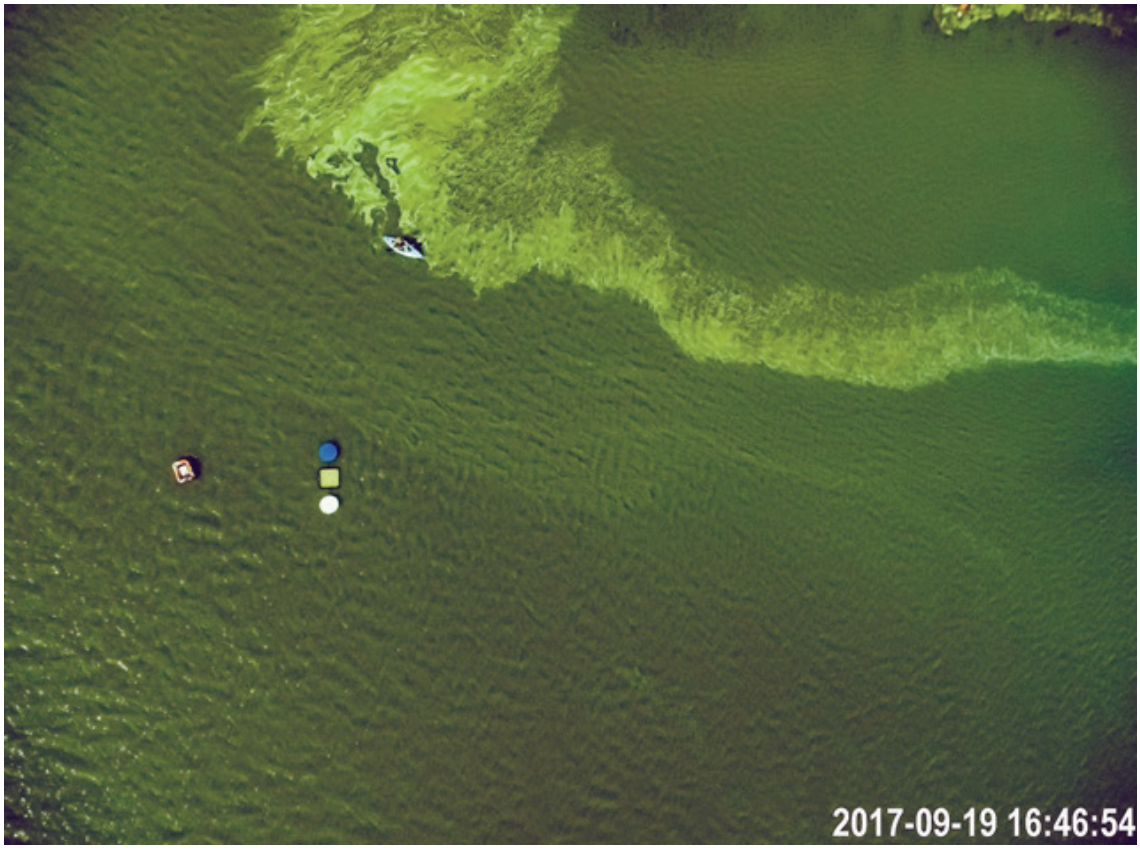

Environmental Laboratory

The US Army Engineer Research and Development Center (ERDC) solves the nation's toughest engineering and environmental challenges. ERDC develops innovative solutions in civil and military engineering, geospatial sciences, water resources, and environmental sciences for the Army, the Department of Defense, civilian agencies, and our nation's public good. Find out more at www.erdc.usace.army.mil.

To search for other technical reports published by ERDC, visit the ERDC online library at http://acwc.sdp.sirsi.net/client/default.

Dredging Operations and Environmental Research (DOER) Program

ERDC/EL TR-23-4
August 2023

Improving Spatial and Temporal Monitoring of Dredging Operations Incorporating Unmanned Technologies

Justin L. Wilkens, Andrew D. McQueen, and Burton C. Suedel

US Army Engineer Research and Development Center
Environmental Laboratory
3909 Halls Ferry Rd
Vicksburg, MS 39180-6199

Final report

Prepared for US Army Corps of Engineers
Washington, DC 20314-1000

Under Funding Element U451408, Funding account U4349741, AMSCO Code 089500, "Improving Spatial Monitoring of Dredging Operations with Unmanned Systems"

Abstract

The US Army Corps of Engineers (USACE) is responsible for maintaining safe and navigable waterways through the periodic dredging of shoaled sediment from federal navigation channels. While dredging, a portion of the bottom sediments become resuspended creating a sediment plume near the dredging operation. Suspension of sediments during dredging and dredged sediment disposal operations continues to be a primary concern of regulatory agencies charged with the protection of environmental resources. Consequently, almost all dredging projects incorporate some level of regulatory compliance monitoring dedicated to measuring sediment resuspension. For numerous reasons the conventional approach using manned surface vessels to perform compliance monitoring is frequently ineffective in both adaptively managing dredging projects and ensuring true environmental protection. Advancements in unmanned platforms and payload technologies offer new and potentially more robust alternatives to conventional platforms. In this study, the use of unmanned aerial system (UAS) and weather balloon mounted camera imagery was demonstrated, and the use of an unmanned surface vessel (USV) to monitor turbidity in navigation channels and near a dredging operation. The imagery from the UAS and weather balloon were compared to in-situ turbidity measurements in a turbid distributary channel and near a dredging operation, while the USV was used to learn more about in-situ turbidity associated with passing vessels in a navigation channel. The results of the demonstrations show the unmanned technology bundled with off-the-shelf payloads can help to produce evidence-based information through easily interpreted aerial imagery and in situ measurements which can help to inform and manage water quality in areas where sediment plumes are an environmental concern.

Contents

Figures and Tables

Figures

Tables

Preface

This report is part of the larger study, "A New Strategy for Water Quality Monitoring." This project was funded by the US Army Engineering Research and Development Center (ERDC), Dredging Operations and Environmental Research (DOER) program. Dr. Todd Bridges was the DOER program manager.

This report was written under the direct supervision of Mr. Warren P. Lorentz, chief, Environmental Processes and Engineering Division, ERDC Environmental Laboratory (EL); Mr. James Lindsay, chief, Environmental Risk Assessment Branch, EL; and Dr. Jack Davis, acting director, EL.

At the time of publication, Mr. James Lindsay was branch chief, EPR; Mr. Warren P. Lorentz was division chief, EP. The director of ERDC-EL was Dr. Edmund Russo, Jr.; Ms. Sheryl Carrubba was Headquarters USACE acting navigation business line manager; and Mr. Charles E. Wiggins, ERDC-CHL, was the ERDC technical director for Civil Works and Navigation, Research, Development, and Technology Transfer portfolio. This study was conducted for the DOER Program under Funding Element U451408, Funding account U4349741, AMSCO Code 089500, "Improving Spatial Monitoring of Dredging Operations with Unmanned Systems." The technical monitor was Dr. Todd S. Bridges, Office of the Senior Scientist Branch (CEERD-EZS).

The authors would like to thank Mr. Jay Bennet, Mr. Austin Davis, Mr. Morris Fields, Mr. Shae Hammond, and Mrs. Christina Saltus of the ERDC-EL and Mr. Thomas Davis of the US Army Corps of Engineers New Orleans District for providing help in collecting and processing field data and providing unmanned aerial system (UAS) services; Mr. Michael Ramirez, Mr. Charles Ellis, and Mr. Charles McKenzie of the ERDC Coastal and Hydraulics Laboratory (CHL) for help in collecting data and providing unmanned surface vessel services; and Mr. Brian LeBoeuf and Mr. Jeffrey Corbino of the US Army Corps of Engineers New Orleans District for providing logistical support in the field.

COL Christian Patterson was commander of ERDC, and Dr. David W. Pittman was the director.

1 Introduction

The US Army Corps of Engineers (USACE) is responsible for maintaining safe and navigable waterways through the periodic dredging of shoaled sediment from federal navigation channels. While dredging, a portion of the bottom sediments become resuspended and create a sediment plume near the dredging operation (i.e., excavation, transit, and placement of sediment). The sediment plume is often described through spatial and temporal measurements of turbidity (an optical measurement of cloudy water), total suspended sediment concentrations (TSS, mg/L), sedimentation rate (mg/cm^2/d), and underwater light concentrations (mol photons/m^2/s) all of which can help predict the potential impacts on nearby aquatic organisms (e.g., Jones et al. 2019; Clarke and Wilber 2008). Assessment of the plume's spatial extent is important when complying with water quality regulations at the dredging and placement sites (Reine et al. 1998). At many dredging operations, plume characterization primarily focuses on the measurement of turbidity (nephelometric turbidity units, NTU) and to a lesser extent TSS (Puckette 1998; Clarke and Wilber 2008). Evaluations of monitored turbidity plumes often suffer from relatively few spatiotemporally limited turbidity samples collected from manned vessels and there are often considerable time intervals between sampling events. Conventional monitoring can provide higher resolution measurements, but such field-monitoring programs are rigorous, time-consuming, and prohibitively expensive. Therefore, there is a need to evaluate emerging remote sensing technologies such as small unmanned aerial systems (UAS) and small unmanned surface vehicles (USV), as alternative or supplemental monitoring methods (Curran and Novo 1988; Binding et al. 2005; Dekker et al. 2001; Dörnhöfer and Oppelt 2016; Kutser et al. 2007).

1.1 Background

Recent advancements in relatively low-cost UAS platforms offer the potential to fill data gaps by providing fine scale remote sensing information, especially for short-term events such as a dredge plume near a sensitive habitat. Recent advances in unmanned technologies offer accurate and programmable navigation capabilities coupled with miniaturized sensors (e.g., LiDAR, color sensors [RGB], near-infrared reflectance [NIR], Hyperspectral) to potentially allow project managers more options to collect

high resolution data previously unattainable with other technologies. Similarly, to improve accessibility and resolution of monitoring near dredge operations, technologies such as USVs are platforms on which sensors can be mounted to perform environmental monitoring (Dunbabin and Grinham 2010; Steimle and Hall 2006). There is a particular interest in the application of USV crafts which are shallow draft and capable of accessing shallow water habitats with water depths < 1 m. These USV platforms potentially offer the capability to measure high spatial and temporal resolution of water quality due to their flexibility as sensor platforms and mobility (e.g., Mogstad et al. 2019; Liu et al. 2016). However, as many of the commercially available USV platforms designed for environmental monitoring are relatively new (Liu et al. 2016), demonstrations are needed to discern the practical efficacy of these applications for monitoring suspended sediment following anthropogenic activities (e.g., dredging and vessel wake). The advancements in unmanned technologies over the past several years provides an opportunity for the USACE to improve monitoring and surveying activities while also improving worker safety and reducing costs. Thus, opportunities to integrate these new technologies into existing dredge monitoring programs and surveys continue to grow.

1.2 Objective

In this study, demonstrations were conducted to examine the efficacy of using unmanned technologies for monitoring sediment plumes and how this can be incorporated into dredge monitoring programs. Unmanned technologies, which included both off-the-shelf and custom-designed solutions, were utilized to gather data and provide insight into the turbidity plumes that were expected to occur around an operating dredge.

1.3 Approach

Three unmanned technologies were employed to monitor or survey turbidity and TSS: a commercially available UAS, a tethered weather balloon, and a custom-built radio-controlled USV. The UAS images were used to demonstrate a simple method to survey water turbidity in a distributary channel near the outlet of the Atchafalaya River. A weather-balloon mounted camera was used to monitor water turbidity and TSS in a shallow coastal shoreline exposed to a cutterhead suction dredge sediment plume. Finally, the USV was used to monitor the effects of ship traffic on water turbidity and TSS in the Calcasieu River and Pass navigation channel.

2 Survey of Water Turbidity in an Atchafalaya River Subdelta Distributary Channel using a Small Unmanned Aerial System

To learn more about sediment transport in the Atchafalaya River, observations and measurements of suspended sediment plumes have been studied previously using satellite reflectance measurements (Shi and Wang 2009; Walker and Hammack 2000; Wells and Kemp 1981; Matthews 2011). While this method provides reliable measurements, remote sensing applications using satellite, as well as manned flight and in situ methods (e.g., measurements from manned vessels) may not be efficient. For instance, the coarse spatial and temporal granularities of satellite imagery limit the capability to monitor relatively short-term sediment plume events. Further, cloud obscuration can make imagery collected by satellite or manned flight unusable. Manned aircraft provide higher spatial and temporal resolution imagery, but expensive image acquisition and operating costs make this option impractical on a routine basis. Monitoring from manned vessels can collect high resolution and reliable measurement but often suffer from relatively few spatiotemporally limited turbidity samples and there are often considerable time intervals between sampling events.

In this context, the use of small UASs has potential to fill in the gaps of data, especially for short-term events and are generally an inexpensive alternative (Watts et al. 2010). Many UASs are a lightweight aircraft (<25 kg) capable of manual, assisted, or semiautonomous flight. The UAS flies at lower elevations (<120 m) and collect images with higher spatial and temporal resolution (e.g., <5 cm/pixel, 60 min revisit time); therefore, UASs can compete with traditional mapping solutions by offering a new high-resolution perspective (Küng et al. 2011).

The objective of this research task was to estimate turbidity levels in an Atchafalaya River subdelta distributary channel below Morgan City, Louisiana. To achieve this objective, a UAS carrying a consumer grade digital camera was used to acquire turbidity reflectance data of a turbid distributary channel along with concurrently collected in situ water samples. Georeferenced images of turbidity were integrated with

geographical information system (GIS) to map the test area with a simple relative turbidity classification which can provide utility to monitoring suspended sediment plumes at larger spatial scales then manned vessels and can be easily repeated over the same area or expanded to monitor larger areas.

2.1 Methods

2.1.1 Demonstration area

The demonstration area was in the Amerada Pass (29.4496°N, 91.3377°W), a distributary channel along the west side of the outlet of the Atchafalaya River main channel south of Morgan City, Louisiana (Figure 1). The Atchafalaya River is the largest distributary of the Mississippi River and features a prograding delta. The river is part of a deltaic system composed of many low gradient distributary channels and interdistributary islands. The subdelta area is fed by the Atchafalaya River which carries a portion of the Mississippi River's water and all water entering from the Red River. Flow entering the Atchafalaya River from the Mississippi River is controlled by the Old River Lock built in 1963 to prevent the Mississippi River from turning into the Atchafalaya River channel.

Turbid water enters the Gulf of Mexico from the Atchafalaya River and flows in a westerly direction in most cases and is easily visible from satellite and manned aircraft (Walker and Hammack 2000). Wells and Kemp (1981) reported total suspended sediment concentrations from 200 to 400 mg/L within the Atchafalaya Bay. Water turbidity levels reported at the Morgan City US Geological Survey water quality monitoring station ranged from 9.5 NTU (minimum) to 339 NTU (maximum) with an average turbidity of 70.4 NTU between 2014 and 2020. During monitoring, the Amerada Pass received primarily deposited sediment inputs from the Atchafalaya River.

Figure 1. Map of Amerada Pass, a distributary channel near the mouth of the Atchafalaya River, south of Morgan City, Louisiana. The *left* inset provides a map of the US, and the *right* inset shows the mouth of the Atchafalaya River. (Satellite photo: Google Earth).

2.1.2 Unmanned aerial system

The survey of turbidity in the Amerada Pass was completed using the commercially available eBeeRTK (senseFly, Switzerland, sensefly.com) fixed-wing drone (Figure 2) equipped with a consumer grade digital camera. The eBee airframe consists of a foam fuselage containing the electronics, built-in autopilot, and camera, detachable wings, and a rear facing electric motor (96 cm wingspan; weighs approximately 0.73 kg including camera and battery). The eBee is equipped to receive position updates via the Global Positioning System (GPS) and Global Navigation Satellite System (GLONASS). The reported absolute horizontal and vertical accuracy without ground control points (GCPs) is 3 cm and 5 cm, respectively (Roze et al. 2014). GCPs are natural features on the Earth's surface or introduced features (e.g., white bucket lid targets) of known locations and can be used to increase the accuracy of geo-referenced image data to centimeter-level accuracy. Because the survey occurred over moving water and because a turbidity plume is dynamic in nature, achieving high accuracy (i.e., centimeter-level accuracy) with GCPs was not a requirement for this demonstration. The distributary channel was also in a remote, hard to access area making GCPs more impractical.

Figure 2. SenseFly eBeeRTK fixed-wing drone used to acquire aerial images. (Photo by Justin Wilkens.)

2.1.2.1 Payload

The eBee payload was a Canon S110 NIR sensor (Canon S110 Near-infrared [NIR] 12-megapixel, Canon, Tokyo, Japan; weight ≈ 180 g; size 98.859 × .026 × .9 mm). This sensor acquires images in the visible (green 550 nm; red 625 nm) and NIR (850 nm) spectrum. SenseFly modified the camera to allow the autopilot to control image acquisition based on user inputs made in the ground station software. To prevent blurred images caused by vibrations, SenseFly programmed the eBee autopilot to stop the electric motor briefly to stabilize in a level attitude prior to triggering the camera. The eBee then resumes the programmed flight path. The approximate ground resolution at 100 m is of 3.5 cm/pixel.

2.1.2.2 Ground control station

SenseFly software, eMotion, was used to plan and control the survey of turbidity from a laptop. The flight was programmed to systematically cover the demonstration area with 75% lateral and longitudinal overlap of images at an altitude of 120 m. The image overlap used in this demonstration was defined by operational capabilities of the equipment. Recommendations of 75% longitudinal overlap and 60% lateral overlap have been suggested, but at the time of this demonstration there was no globally accepted standard on the best overlap and the requirements also depend on what target(s) are being imaged (Rasmusset et al. 2014). Images were georeferenced, whereby, the onboard GNSS and inertial measuring unit determined the position and orientation of the camera. The flight software provided the capability to monitor progress of the flight in real time and included information about image acquisition, position, telemetry status, time remaining in flight, battery voltage, speed, altitude, and other system information. After hand launch, the UAS circles at a specified altitude until initiation of the survey mission by the UAS pilot at which time the UAS enters an autonomous flight mode and carries out the mission. To land, the UAS autonomously returns to the launch location, descends, and skid-lands. Deployment and retrieval of the UAS occurred in a clearing near the distributary channel.

2.1.3 Water quality

Within 30 min postflight, in situ water samples (500 ml) were collected to correlate with UAS images. Because of low water currents, wind (≈0.5 m/s), and relatively homogenous turbidity conditions, the samples

were considered representative of the acquisition time of the aerial images. Within the UAS image acquisition area, collection of water samples occurred at 14 sites. Sampling locations were determined in the field and were considered representative for monitoring the demonstration area (<1 km^2) mapped by aerial images (Figure 3).

Each sampling location was marked using a GPS (Trimble SPS 5800, Sunnyvale, California). Plastic bottles (250 ml) rinsed with water from each location were refilled with water collected near the surface (i.e., top 5 cm). The samples were kept at 4°C and later used for laboratory analysis of turbidity and TSS. The post sample laboratory process used a turbidimeter (Hach 2100Q, Loveland, Colorado) to measure turbidity of the hand-collected samples. Values used represented the mean of three turbidity measurements taken from each sample (Table 1). For TSS, the water sample was manually mixed and then a wide-mouthed pipette was used to collect a 100 ml sample. The samples were transferred to a vacuum filter apparatus and the pipette was rinsed with deionized water to ensure all sediment was transferred. The preweighed filters and contents were dried at 105°C overnight then reweighed to the nearest 0.0001 g using an analytical balance (MS104TS, Mettler Toledo, Columbus, Ohio).

Figure 3. Map of sites (n = 14) where water was collected from the Amerada Pass, a distributary channel near the mouth of the Atchafalaya River, south of Morgan City, Louisiana, on 22 June 2016.

Table 1. Results of water quality measurements taken of samples collected near the water surface (top 15 cm) in a distributary channel near the mouth of the Atchafalaya River south of Morgan City, Louisiana, 22 June 2016.

	Laboratory		Field Location and Time		
Sample	Turbidity (NTU)	TSS (mg/L)	Latitude	Longitude	Time
1	15.7	19	29.448	-91.338	11:49:32 AM
2	16.1	18	29.449	-91.338	11:53:02 AM
3	24.3	26	29.449	-91.338	11:54:12 AM
4	49.8	53	29.450	-91.339	11:57:02 AM
5	49.1	54	29.450	-91.340	11:58:12 AM
6	48.1	50	29.451	-91.340	12:00:07 PM
7	47	52	29.451	-91.341	12:03:27 PM
8	47.4	58	29.450	-91.339	12:06:07 PM
9	49.9	60	29.450	-91.338	12:08:42 PM
10	54.3	76	29.449	-91.337	12:11:42 PM
11	51.8	66	29.449	-91.335	12:14:27 PM
12	47.9	59	29.450	-91.334	12:16:57 PM
13	48.8	58	29.449	-91.334	12:19:37 PM
14	50.5	58	29.449	-91.333	12:21:42 PM

2.1.4 Data processing

After the UAS survey, Pix4Dmapper (Pix4D, Switzerland) photogrammetry software was used to process the images to create an orthomosaic image of the demonstration area. The geotag provided by the UAS autopilot determined image position and orientation. This post image processing was robust in that it provided a “one click” solution. The orthomosaic, overlaid with water sample locations, was used to create a map and a color bar to display the relative concentration estimates of turbidity of the pixels representing the channel. The Semi-Automatic Classification Plugin for Quantum GIS created a relative turbidity classification by manually selecting and classifying training areas with different spectral signatures using a manual delineation (Congedo 2016).

2.2 Results and discussion

One 25 min flight conducted 22 June 2016, acquired images of the distributary channel over a survey area of approximately 50 ha with a ground resolution of 5.2 cm/pixel. Weather conditions were wind speed of 0.5 m/s from the south-southeast with a maximum wind speed of 5 mph; visibility 10 miles; and scattered clouds (above flying area). Turbidity near the water surface ranged from ≈15–55 NTU. Acquired images were successfully georeferenced and used to create an orthomosaic image (Figure 4). A map created by classifying the orthomosaic image visually estimated water quality parameters based on a color scale (Figure 5).

Figure 4. Georeferenced orthomosaic created with near infrared aerial images of the distributary channel near the mouth of the Atchafalaya River south of Morgan City, Louisiana, 22 June 2016.

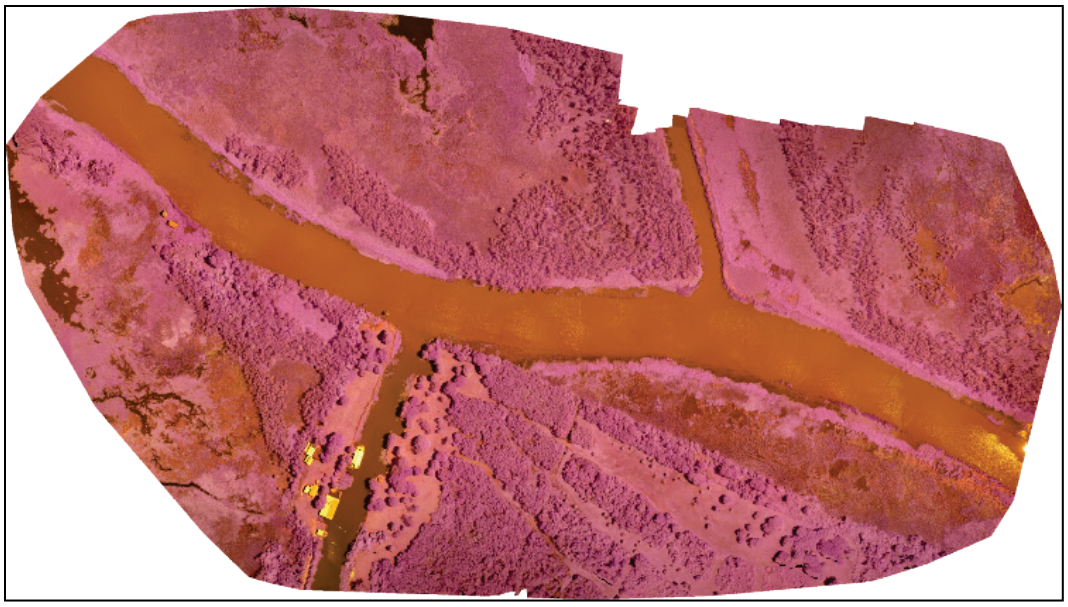

Figure 5. Map of estimated turbidity created after in situ water samples were correlated with aerial images of a distributary channel near the mouth of the Atchafalaya River south of Morgan City, Louisiana, 22 June 2016.

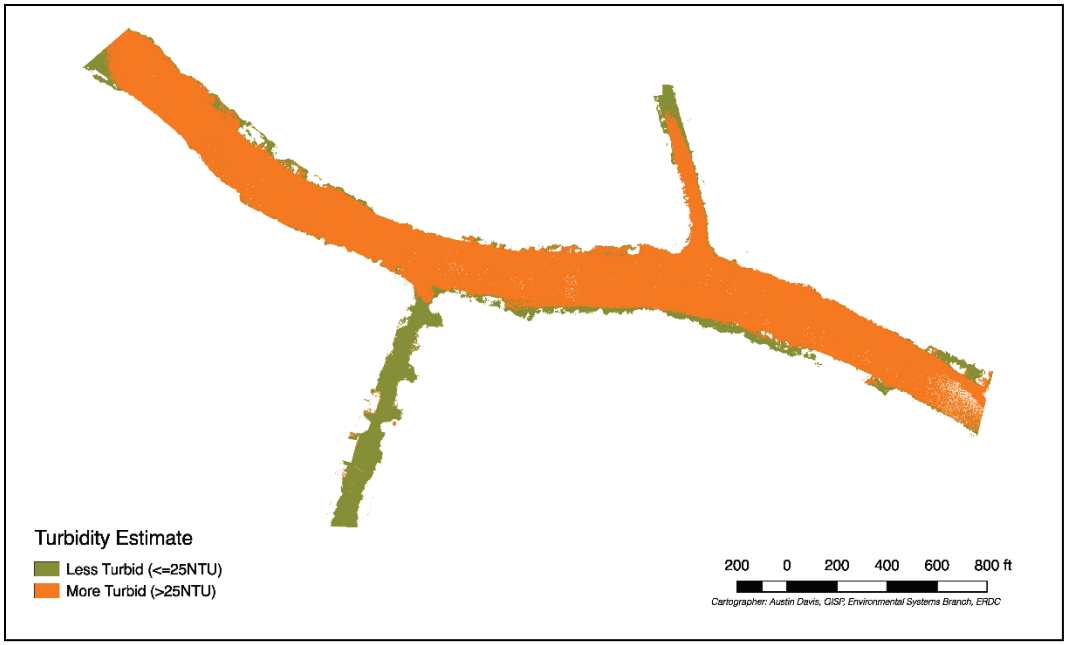

Combining the map overlay with in situ water samples allowed for evaluation of turbidity and TSS concentrations over a large area. Ideally, creation of several training areas with different spectral signatures is desirable when considering the spectral variability possible for different turbidity levels. Without a color reference to help spectrally calibrate an image, precise and accurate measures of turbidity were not possible. However, observations of the data suggested that regions of lower spectral intensity in the waterway represented lower NTU values. This pattern was evident in the water samples collected at various locations. Segmenting the intensity values into two categories produced a map, such that areas classified within the lower intensity category were estimated to represent areas of turbidity below 25 NTU. The high ground resolution (5.2 cm/pixel) offered sufficient contrast for areas with relatively homogenous turbidity (i.e., <25 or >25 NTU). Figure 6 displays the workflow for developing the UAS remote sensing application.

Figure 6. Flowchart of the steps used to generate the relationship between turbidity and aerial images using UAS technology.

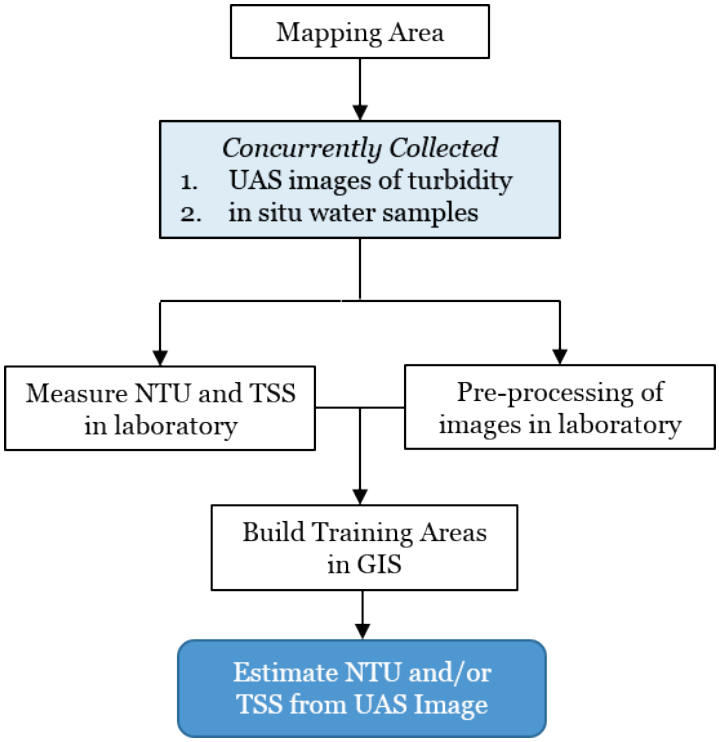

When visually estimating turbidity with UAS images, it is important to correlate turbidity levels with spectral signatures to predict related water quality parameters. If the turbidity-spectral signature relationship is weak or spectrally uncalibrated, it may only be useful for establishing general trends and will be unable to provide an accurate visual estimate. To develop a more accurate characterization and classification system for turbidity measurement using UAS imagery, placement of subsurface spectral calibration panels within a subset of the images could help to perform spectral calibration. Further, the calibration panel could be associated with a turbidity sensor to help predict turbidity across the geographic space. However, even when successfully calibrated, the data tend to be site specific and require daily calibration (see Lui et al. 2003). Therefore, in many situations daily flights and in situ sampling are likely required to build useful applications. Automation of these processes with, for example, turbidity data loggers could help decrease effort. Currently, the discrimination of turbidity levels using UAS images does not provide real time turbidity monitoring data as compared to data collected in real time in the field from a manned vessel and data loggers. Depending on the intended operational use of the UAS images, the resulting orthomosaic may be more useful for determining large scale impacts which in turn can

help to improve overall dredging operations, versus real-time, but spatially limited measurements from a manned vessel used for short-term operational management triggers and corrections.

Although there may be limitations to real time data retrieval, UAS still have the potential to increase the spatial assessment of sediment plumes in comparison to conventional manned vessel methods while providing the necessary accuracy (Vogt and Vogt 2016). In terms of a dredging operation, the movement of plumes and dissipation over space and time is important for predicting potential impacts associated with dredging. There are challenges in characterizing dredge plumes because of their variable nature. The nature and extent of a dredge plume is mostly the result of the dredge type, hydrodynamics, and sediment characteristics. A plume may exhibit systematic patterns of distribution influenced by local environmental conditions from the onset of the plume to resettling; but such conditions may only persist for short periods before changing. Therefore, it may be challenging, for instance, to collect water samples representative of the aerial images. However, even if calibration fails to provide an accurate turbidity measurement, georeferenced images can still provide relative estimates as evidence of the plumes' spatial scale and proximity to sensitive habitats that manned vessels could not otherwise easily obtain. This information could support better-informed best management practices for dredging operations, especially if additional steps to calibrate the spectral signature of images within situ water samples is applied.

2.3 Summary of survey of water turbidity in an Atchafalaya River subdelta distributary channel

During the demonstration, it was observed that high-resolution water surface images obtained from UAS could be used to differentiate turbidity levels quickly and easily, provided they are relatively calibrated to in situ water samples. However, the UAS image sensor's ability to penetrate the water column is subject to the clarity of the overlying water which in some cases could limit its application to shallow water habitats or the immediate water surface. Whether or not this technology would be useful in a dredging application depends on several factors, such as the dredge type, hydrodynamics, and sediment characteristics that determine the location of the plume in the water column. If a large portion of the sediment plume occurs near the bottom of the channel, the UAS application may be limited, especially if the overlying water clarity is low. However, if

dredging occurs in exceptionally clear water, such as in Hawaii, or if a portion of the plume is readily visible near the surface, then this technology will help improve the spatial and temporal monitoring of dredging.

3 Estimating Turbidity near a Dredge Operation using a Weather Balloon-Mounted Camera

The improvement of UAS platform technologies allows the opportunity to collect imagery with high spatial and temporal resolution, however, State laws, the Federal Aviation Administration (FAA; Small Unmanned Aircraft Systems 2020), and US Army rules (US Department of the Army 2018) governing UAS operations can hinder their use in some situations. Deploying remote sensing technologies using tethered airships may be more reliable and operations repeatable in many project settings because they are less restricted by FAA and US Army regulations. This option can potentially produce desirable high spatial and temporal resolution of the optical water properties (e.g., turbidity) over a long monitoring period (e.g., hours to days). The temporal variability of turbidity near a coastal dredging operation is influenced by tides, prevailing winds and currents, and river flow which can result in a continuous movement of water, thus, a longer monitoring period is an attractive alternative to consider (Doxaran et al. 2002). As with UAS operations, in situ water grab samples concurrently collected with spectral reflectance data helps to build an empirical relationship but is often inadequate to represent a dynamic system if too few samples are collected. Alternatively, an automated turbidity monitoring station synched with image collection may result in a more practical approach. In comparison to a UAS, a tethered airship is limited to a smaller monitoring area, but potentially well suited for monitoring ecological sensitive areas that may benefit from continuous measurements during dredging operations (e.g., oyster reef, seagrass, and coral reef). Additionally, the tethered airship provides an opportunity to collect data over longer periods of time which can provide insight into useful information about the temporal variability of spectral reflectance correlated to TSS or NTUs.

The research task objective was to use remotely sensed reflectance in the visible spectrum to estimate the concentration of suspended sediments within an active dredge plume. To achieve this objective, a low-cost monitoring system was developed consisting of a weather balloon-mounted consumer grade digital camera to acquire turbidity reflectance in the visible bands (400–700 nm) of a shallow coastal area affected by a pipeline discharge of dredged sediment.

3.1 Methods

3.1.1 Demonstration area

The demonstration area was in the Gulf of Mexico immediately west of a rock jetty (29.7300° N, -93.0129° W) which extended from the mouth of the Mermentau River, south of Grand Chenier, Louisiana (Figure 7). This area is part of the Chenier Coastal Plain which is characterized by low gradient muddy shorelines or mud flats with an abundance of sediments deposited from tides and rivers (Wells and Kemp 1981). A cutterhead pipeline dredge, Ingenuity, excavated sediment from the mouth of the river near the end of the west rock jetty. Dredged sediment was discharged into the shallow coastal waters of the Gulf of Mexico via a pipeline positioned on top of, and perpendicular to, the west rock jetty. The combination of primarily south, southeast winds, and the jetty, resulted in surface water currents that moved southeast into the corner where the jetty and shoreline met and then continued west along the shoreline. Observations confirmed that a portion of the dredge sediment plume migrated along this path and extended down the shoreline. Based on the sinuous path the turbidity plume traveled, the turbidity monitoring site was approximately 0.75 km from the discharge pipe where the sediment plume originated. At the monitoring site, the balloon was tethered and launched ≈30 m seaward of the shoreline over water depths that ranged 1–2 m. The demonstration area was subjected to primarily dredge plume inputs and naturally deposited sediment inputs from Mermentau River along with low wave energy and tidal influences.

Figure 7. Demonstration area located in the Gulf of Mexico near the mouth of the Mermentau River, south of Grand Chenier, Louisiana (Satellite photo: Google Earth TerraMetrics 2017). The *red circle* shows the general location where the balloon was deployed, while the *black line* shows the general location of the cutterhead dredge pipeline discharge. Based on visual observations of the turbidity plume while at the site, the plume was manually added to the photo to demonstrate the plume pattern. The inset is a 3D view of the balloon deployment.

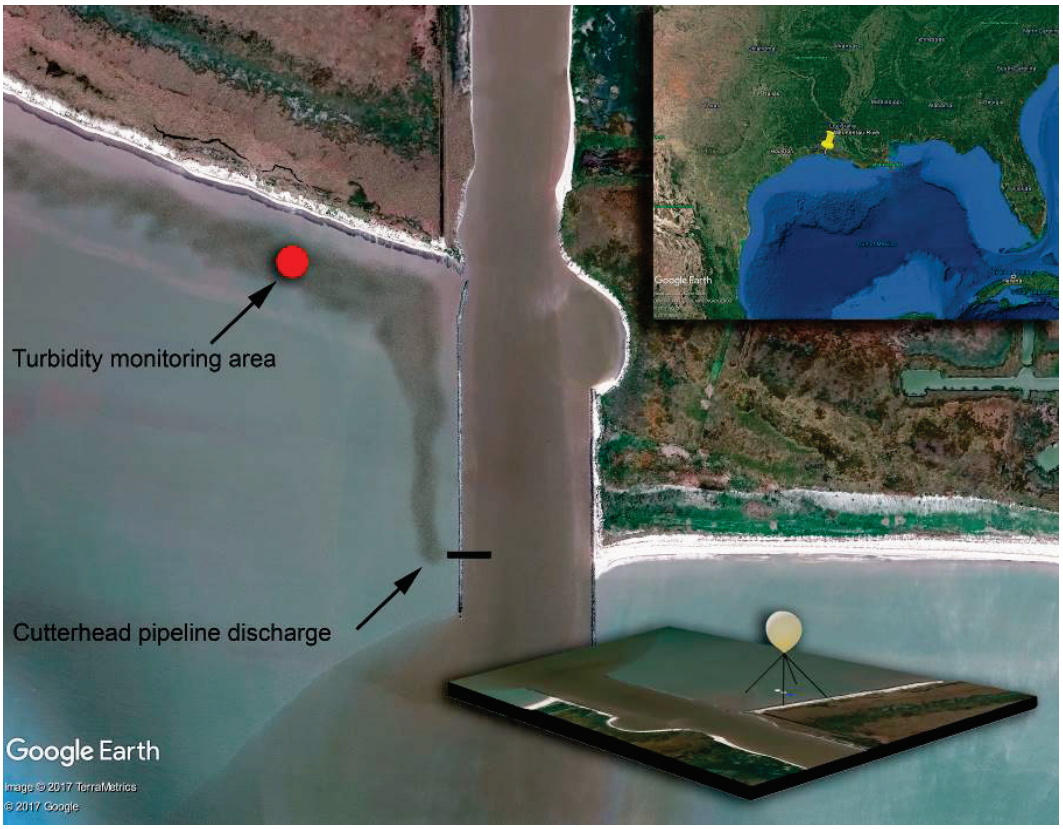

3.1.2 Digital camera

A consumer-grade digital camera sensor (Survey2, Visible Light RGB, MAPIR, San Diego, California) powered via USB by external battery, captured images in the visible spectrum (400–700 nm). The camera (16 megapixel) sensor achieved a ground sample distance of 4.05 cm per pixel at 120 m above ground level (lens optics: 82° HFOV [23 mm] f/2.8 aperture [fixed], -1% extreme low distortion [nonfisheye] glass lens). The deployed camera settings included

- 4:3 crop,
- RAW+JPG acquisition,
- shutter speed 1/1000,
- time lapse 5 sec,
- exposure value compensation +0.0,
- ISO-50,

- color normal,
- contrast normal,
- sharpness normal,
- metering average, and
- single image capture mode.

Because the camera sensor uses a Bayer filter, there are twice as many green photosensors as there are red and blue, so a custom white balance (R1, B1) was used to enhance the capture of green colors at the green photosites on the sensor to increase the likelihood of detecting changes in turbidity.

3.1.3 Weather balloon

A helium inflated weather balloon (1,500 g, KCl-1500, Kaymont Consolidated, Melbourne, Florida) achieved a 2 kg lift force and successfully deployed the camera mount. The camera mount consisted of Styrofoam (Smoothfoam Half Balls-15.24 cm, Hobby Lobby, Oklahoma City, Oklahoma), where the camera, video downlink, battery, and other small accessories fit inside (≈ 950 g total weight). The camera mount hung from lines as part of a modified Picavet system (Picavet 1912) attached to a square supporting frame. The weight of the camera mount caused it to settle into a relatively level position and resulted in approximately vertical photographs (Figure 8). The Picavet system attached to a swivel which attached to the neck of the balloon by a 3 m length of cord (3 mm diameter nylon cord). The swivel helped to compensate for balloon twist. Each corner of the square aluminum support frame connected to a tether. Each tether was secured to a metal fence post and enough tether was released to allow the balloon to float in a stationary position approximately 45 m above the water surface.

Figure 8. Photos of modified Picavet system (*left*); shoreline and mudflat (*middle*); balloon deployment (*right*). (Photos by Justin Wilkens.)

3.1.4 Reflectance targets

To enhance the spectral reflectance sensitivity a white reference target floating on the water surface and a white reference target submerged below the water surface were situated to be visible in each image. The reference target submerged underwater consisted of three layers of Tyvek glued to a 0.91 m^2 acrylic sheet (1.27 cm thickness). The acrylic sheet was used because it provided a rigid flat surface for attaching Tyvek, low flexibility, and remained submerged by its own weight. In each corner of the acrylic sheet, a 2.54 cm hole was drilled, and a PVC bulkhead fitting was installed. The target was suspended from a 0.91 m^2 floating platform constructed of 3.81 cm diameter PVC pipe, by chain. At each corner of the platform a chain was attached by a marine grade hose clamp. At each platform corner, the free hanging chain was then pulled through each bulkhead fitting on the acrylic sheet reference target. On each chain, a carabiner was clipped through a link to set the depth at which the reference target would remain submerged under the water surface below the platform. For this demonstration, the target was submerged 7.62 cm below the water surface.

The white reference target floating on the water surface also consisted of three layers of Tyvek glued to a 0.91 m diameter circle cut from a white fiber reinforced polymer sheet. The surface reference target was attached by Velcro to 8.89 cm diameter noodle foam floats which were installed on a 0.45 m^2 floating platform constructed of 1.27 cm diameter PVC pipe. The noodle foam floats were used for floatation and to keep the reference target several centimeters above the water surface to prevent water from lapping onto the target. The platform holding the surface reference target was attached to the platform hanging the submerged target by a 0.61 m long PVC piece and hose clamps. All visible PVC pipe was spray painted black with satin finish to reduce interference with reference targets.

3.1.5 Turbidity monitoring

The NTU sensors were mounted to the reflectance target platforms and positioned about 7.62 cm below the water surface to collect NTUs near the water surface which would better represent reflectance values. This measurement depth was chosen because the radiance penetrates only the top few millimeters of the water column before being absorbed or reflected. An optical backscatter turbidity sensor (OBS-3+, 0–1,000 NTU,

Campbell Scientific) was mounted to the submerged target platform to collect NTU readings prior to the turbidity plume moving over the submerged target. Another turbidity sensor was mounted on the white reference surface target platform to measure turbidity in a blank area adjacent to the target. Approximately 2 m separated the turbidity sensors. The turbidity sensors were both connected to a data logging device which collected measurements every ten seconds. The data logging computer clock was synchronized with the camera clock so that date and time stamps could be used to produce concurrently measured NTU and reflectance data.

3.1.6 Data processing

No adjustments were made to the images post acquisition. The JPEG images were selected and processed using a Python script (PSF 2018). Raw images were not analyzed but would likely exhibit the same pattern but with less uncertainty. Regions of interest (ROI) were automatically digitized in each image to select pixels from the white reference surface target, white reference submerged target, and the open water area adjacent to the white surface target. A circle marked all the pixels belonging to the ROI over each target. For each ROI, the mean RGB spectral reflectance data were extracted by adding the red, green, and blue values and each divided by the number of pixels in the ROI. (e.g., range 0–255 for 8-bit color channel). Then, a relative reflective index was calculated from equation 1 as given below:

$$Relative\ reflective\ index = (RGB_{target})/(RGB_{surface}) \quad (1)$$

where RGB_{target} is the sum of the RGB of the desired target in the image and $RGB_{surface}$ is the sum of the RGB of the white reference surface target. A regression was used to explore the relationship between the relative reflective index determined for the submerged and open water targets and turbidity.

3.2 Results and discussion

The weather balloon was successfully deployed on 19 and 20 September 2017 to a height of approximately 45 m with a ground sample distance of less than 2 cm per pixel (Figure 9). Weather conditions on the first day were wind speeds of less than 5 m/s with minimal gusts from the south-

southeast, scattered clouds, and max temperature of 31°C. In situ image acquisition and NTU readings started at approximately 1400 hours and ended at 1745 h. Weather conditions on the second day were sustained wind speeds of approximately 5 m/s with gusts frequently exceeding 9 m/s from the south-southeast, scattered clouds with short rain events, and max temperature of 31°C. The balloon and NTU sensors were briefly deployed from approximately 1300 to 1445 hours and then grounded due to wind gusts and rain. When the balloon was tethered in strong winds it was observed the balloon lost its round and more aerodynamic shape and instead became flatter or more convex shaped. The combined effects of increased drag and repeated wind gusts eventually resulted in the balloon altitude suddenly decreasing and sailing downwards nearly into the water. In addition to difficulties with balloon deployment on the second day, there were also numerous negative or zero readings from the NTU sensors because of wave action which repeatedly lifted the sensors from the water. Because of lack of data collection on the second day, only the first day is reported.

Figure 9. Photo from weather-balloon-mounted camera of white surface target, white submerged target, blue surface target, turbidity sensor locations, and a sediment plume approaching the monitoring area.

On the first day, a total of 1,937 images were acquired of which 1,133 images were concurrently acquired (58%) with an NTU measurement and were used for analysis. The mean (± standard deviation) turbidity measurement was 31.3 NTU (±22.1) for the sensor monitoring water near the submerged target and 23.3 NTU (±7.6) for the sensor in the open water area (Figure 10). The turbidity ranged from 11 to 114 NTU for the sensor data combined. These turbidity levels are within a range commonly experienced near a dredging operation. Prior to set up, dredge operations temporarily stopped while the crew repositioned the dredge near the west rock jetty and as a result turbidity concentrations remained relatively constant (20–40 NTU) for the first few hours of sampling. Once dredging operations resumed, a sediment plume was visually observed and eventually a portion of the plume (max 114 NTU) migrated through the sampling area between 1635 and 1650 hours. The turbidity sensor located at the submerged target was subject to more variation and numerous outliers up to approximately 1540 hours at which time the readings appeared more like the other sensor in the open water. These outliers are likely the result of a mounting issue while others could have occurred when a kayak was nearby collecting water samples. A review of the images before, during, and after the outliers confirmed no obvious plume was visible (e.g., > 220 NTU would nearly saturate the visibility of the submerged target).

The NTU peak that occurred when the dredge plume migrated through the sampling area showed similar trends between sensors, but the sensor located near the submerged target measured a higher NTU. It would appear the sensors performed differently, but a closer examination of the images showed the edge of the plume passed through the sampling area, so it is more likely that the sensors saw two different turbidity levels. Because the dredge operations ceased during the first hours of sampling and because no plumes were visibly present in the images prior to the dredge plume beginning at 1635 hours, only the turbidity measured immediately before, during, and after the dredge plume migrated through the turbidity monitoring area (starting at 1600 to 1706 hours) was used to determine if the plume could be detected.

Figure 10. Turbidity (NTU) measured at the white reference submerged target (submerged) and the white reference surface target (open water).

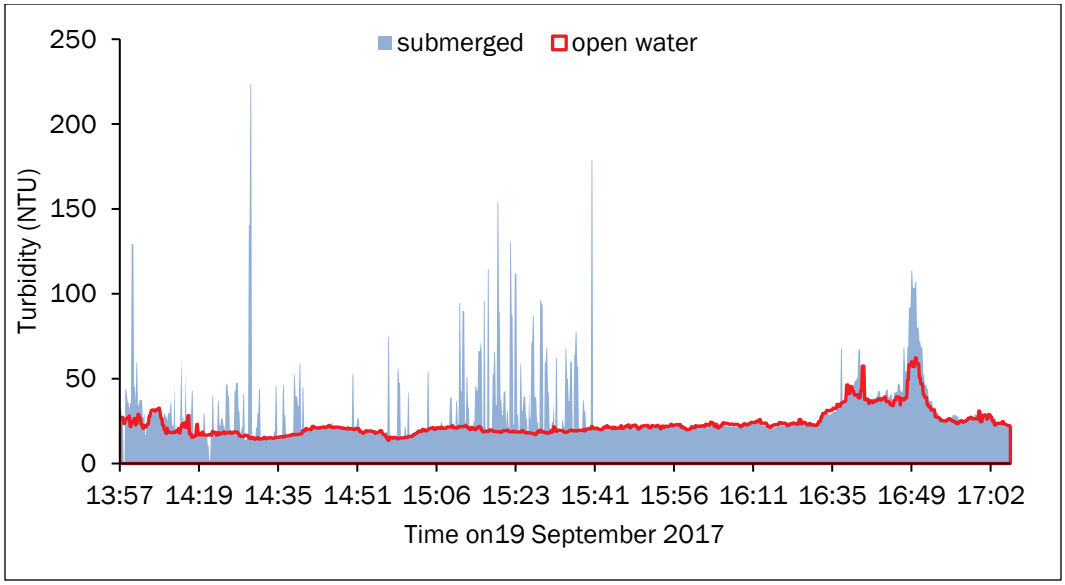

The Python script successfully identified each reflectance target and created ROIs for each in >99% of the images. The remaining images were omitted due to interferences (e.g., camera off target due to wind). The manual camera settings resulted in green colors exhibiting the highest RGB reflectance values (mean, range––255 max value for each 8-bit color channel) for the white surface target (214, 122–242), followed by the submerged target (135, 40–193), and open water (48, 18–85) (Figure 5). The total RGB intensity was greatest for the white surface target, followed by the white submerged target, and last, open water (Figure 11). The total RGB intensity of the white surface (514, 261–694) and submerged targets (298, 82–432) was greatest at the beginning of the sampling period (1357 hours) and noticeably decreased throughout the day as the sun angle decreased. In contrast, Figures 11 and 12 depict the open water RGB intensity (103, 43–196) remaining relatively constant throughout the sampling period with only a small decrease over time which suggests the sensor was near saturation because of environmental conditions in the open water area.

Figure 11. Total RGB intensity measured for the white reference surface target (surface), and white reference submerged target (submerged) and open water adjacent to the surface target (open water).

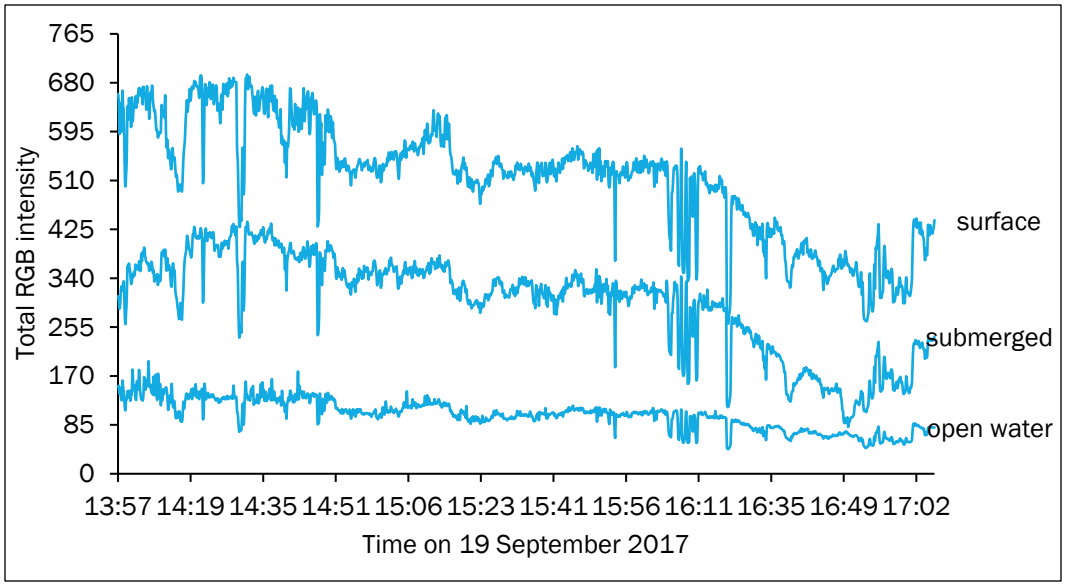

Figure 12. The green color reflectance value of the white reference surface target (surface) and white reference submerged target (submerged) and open water adjacent to the surface target (open water).

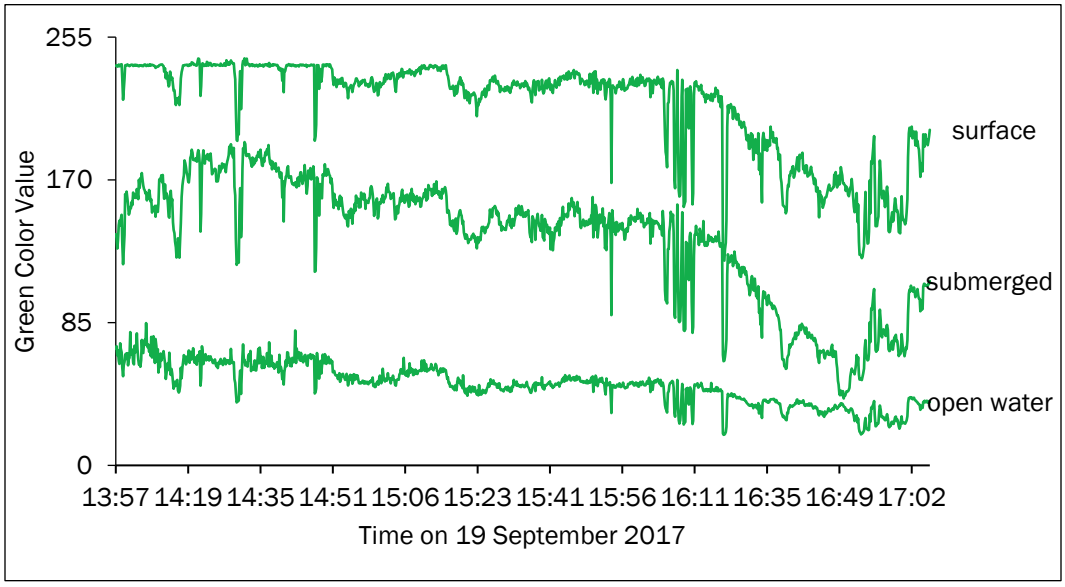

The relative open water reflectance calibration showed no relationship between relative reflectance and turbidity; therefore, under these field conditions, it would be difficult to rely on visible reflectance data as an indicator of turbidity (Figures 13 and 14). Sun glint, clouds, and waves were likely the main environmental factors contributing to the low-quality signal in the open water area (Zeng et al. 2017). Increasing altitudes from

20 to 100 m have been shown to have negligible effects on water reflectance thus balloon altitude likely had little influence on the results (Zeng et al. 2017). When comparing total reflectance values between the reflectance targets, the reflectance of the open water as compared to the white reference target decreased by an average 80% while the submerged target decreased by only 43%. The percent increase in reflectance from open water to the submerged target averaged 188% due to increasing reflectance from the Tyvek. Most of the reflectance values are derived from the water surface, thus an 80% decrease in signal due to environmental factors resulted in reduced signal from which to detect changes in turbidity in open water.

Figure 13. Scatter plot of relative open water reflectance (open water reflectance / white reference surface target reflectance) and corresponding turbidity measurements.

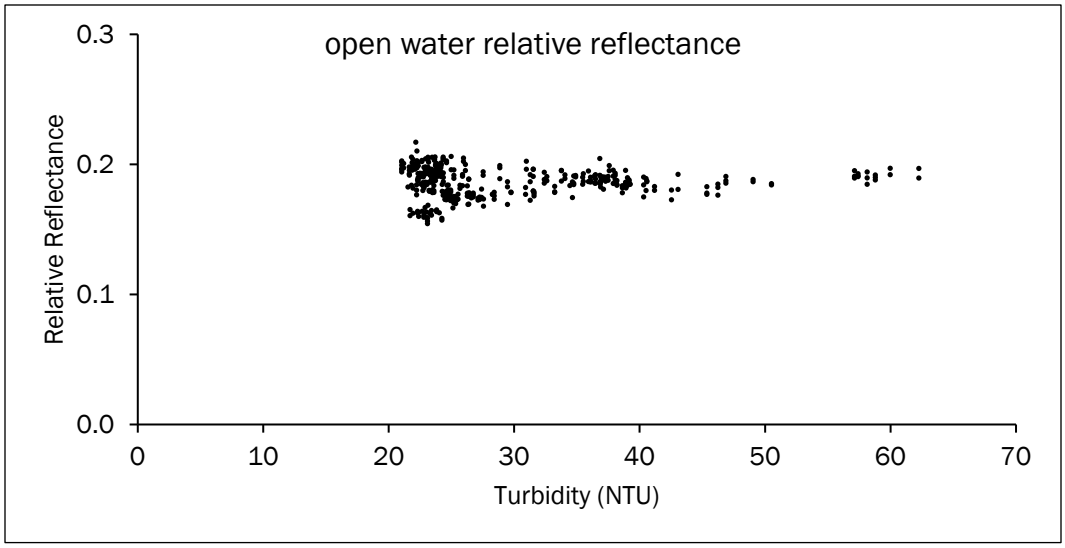

Figure 14. Open water relative reflectance (open water reflectance / white reference surface target reflectance) and corresponding turbidity measurements plotted over time.

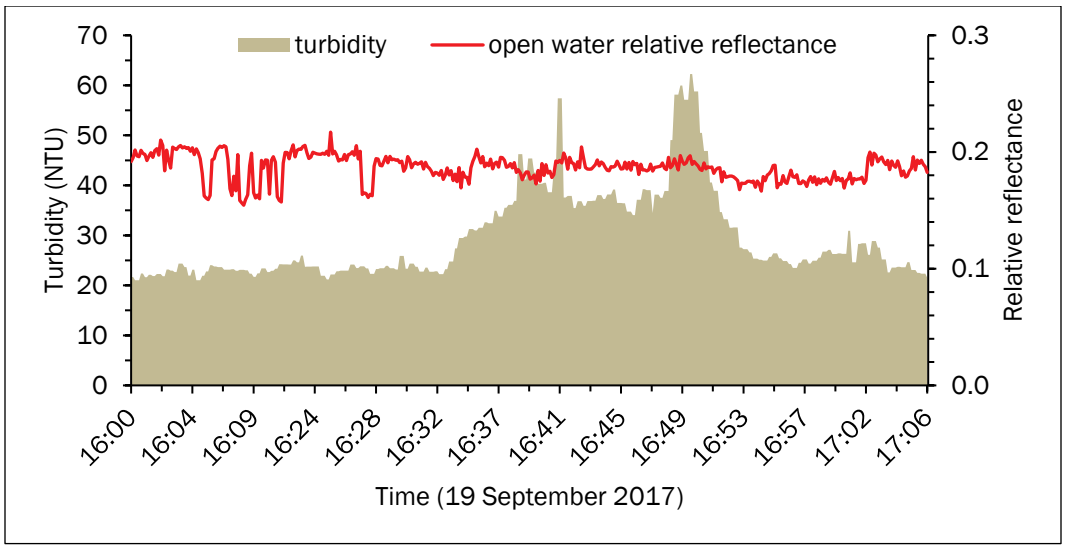

The importance of a white reference surface target and submerged target calibration is demonstrated by the relative submerged reflectance plotted against the turbidity measured at the submerged target (Figures 15 and 16). An inverse logarithmic trend between relative reflectance and turbidity is apparent (R^2 = 0.7953). The use of surface and submerged white reference targets reduced uncertainty when correlated to concurrently measured turbidity and extended the utility of the consumer grade digital camera in a shallow water turbid coastal environment.

Figure 15. Scatter plot of relative submerged reflectance (white reference submerged target reflectance / white reference surface target reflectance) and corresponding turbidity measurements.

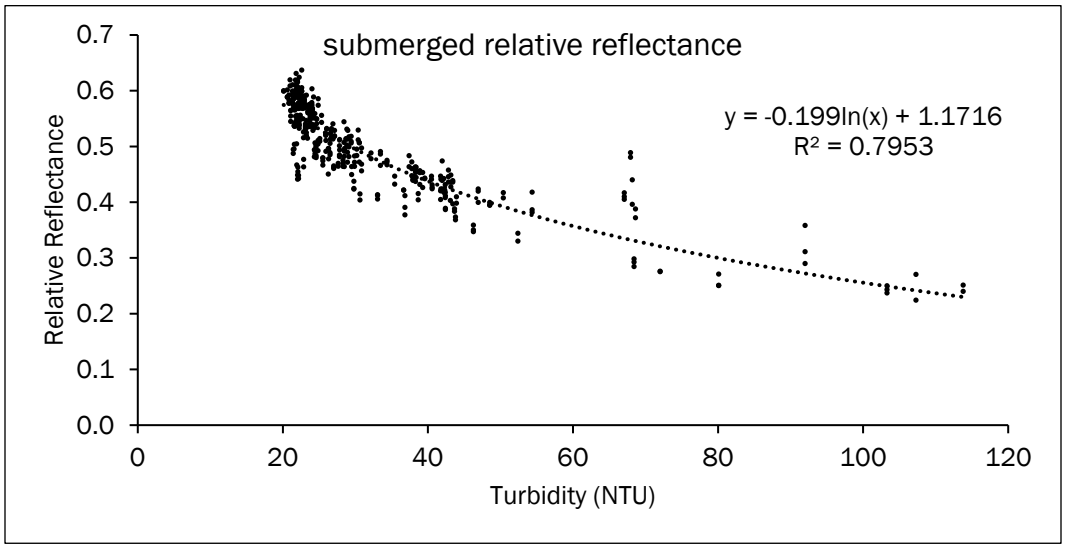

Figure 16. The relative submerged reflectance (white reference submerged target reflectance/white reference surface target reflectance) and corresponding turbidity measurements plotted over time.

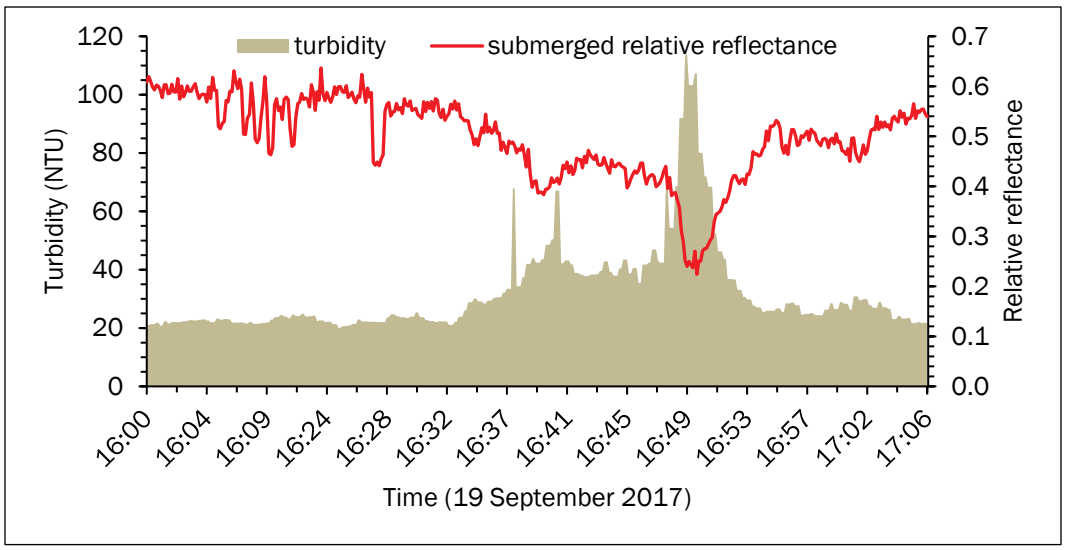

A logarithmic relationship is expected because increasing turbidity would eventually eliminate reflectance values measured at the submerged target. This was observed in a bench scale test performed with the camera prior to field sampling where it was determined that when the white reference target was submerged 7.62 cm below the water surface the reflectance from the target was eliminated when turbidity reached approximately 250 NTU and at 2.54 cm the submerged target reflectance was mostly eliminated at 500 NTU. These bench-scale observations generally support the field results, in terms of anticipated visible spectrum saturation with increasing water turbidity. The combination of the white surface target and the submerged target make it possible to monitor turbidity migrating over the targets using the visible RGB wavelengths within environmentally relevant accuracy and precision up to a saturation point which is dependent on the depth of the submerged target (Haque and Adhikary 2016).

3.3 Summary of estimating turbidity near a dredge operation using a weather balloon-mounted camera

This study successfully created a low-cost turbidity monitoring system using a consumer grade digital camera mounted on a weather balloon to capture turbidity reflectance in the visible bands of a shallow water turbid coastal environment. The study found that using surface and submerged white reference targets improved spectral reflectance and reduced uncertainty in turbidity monitoring and prediction when correlated with

concurrent turbidity measurements. Relying solely on open water RGB did not accurately estimate turbidity. These results support previous research showing a logarithmic relationship between reflectance and turbidity, where spectral sensitivity decreases and eventually saturates as NTU increases. This information can help design and implement low-cost monitoring systems for remotely sensing turbidity plumes, and a more aerodynamic and steerable dirigible could increase reliability.

4 Estimating Turbidity and Suspended Sediment Concentrations using an Unmanned Surface Vehicle

Dredging commonly occurs in shallow waters to deepen or maintain channels to ensure safe and navigable access to ports and harbors. Proximity of dredging to sensitive shallow water habitats (< 2 m water depth; for example, oyster bed, coral reef, fish spawning habitat, submerged aquatic vegetation, etc.) is common and can result in State or Federal resource agencies restricting dredging events to specified time periods known as environmental windows, with the intent to avoid potential ecological risks (Reine et al. 1998; Suedel et al. 2008). Physical impacts such as turbidity, total suspended sediments (TSS; mg/L), and sedimentation are often reported as the main justification for environmental windows (Wegner et al. 2017; Wilber and Clarke 2001; Reine et al. 1998). Thus, monitoring of turbidity and suspended sediment near dredging activities is important.

Monitoring typically occurs from a manned surface vessel or buoy-based turbidity monitoring systems. However, these methods are spatially and temporarily limited and are often not capable of accessing shallow water habitats due to vessel limitations. To improve accessibility and resolution of monitoring these areas, technologies such as unmanned surface vehicles (USV) are platforms on which sensors can be mounted to perform environmental monitoring (Dunbabin and Grinham 2010; Steimle and Hall 2006). For shallow water habitats, there is a particular interest in the application of small (< 2 m length) USVs which are shallow draft and capable of accessing water depths < 1 m. These USV platforms potentially offer the capability to measure high spatial and temporal resolution of water quality due to their flexibility as sensor platforms and mobility (e.g., Mogstad et al. 2019). However, as many of the commercially available USV platforms designed for environmental monitoring are relatively new (Liu et al. 2016), demonstrations are needed to discern the practical efficacy of these applications for monitoring suspended sediment following anthropogenic activities (e.g., dredging and vessel wake).

For the purposes of this demonstration, a custom-built radio-controlled USV outfitted with a turbidity sensor, water sampler, and an acoustic Doppler current profiler (ADCP) monitored wave energy and suspended

sediments. The goal was to demonstrate the USV efficacy for estimating sediment suspension and mobility from vessel wakes by measuring the relationship of suspended sediments (as TSS and turbidity [NTU]) following waves propagated by vessels in the Calcasieu River and Pass, Louisiana (herein referred to as the Calcasieu Ship Channel). To achieve this goal, the research project had three objectives. The first objective was to measure the relative influence of vessel wake on the resuspension of sediments near a shallow wetland habitat. The second objective was to measure the relationship between vessel size and type and resulting sediment disturbances, such as increased turbidity and TSS. Finally, the third objective was to discuss the possibility of developing a USV application for monitoring dredge plumes near sensitive shallow water habitats.

4.1 Methods

4.1.1 Demonstration area

The demonstration area was in the Calcasieu Ship Channel near the mouth of Kelso Bayou, north of Hackberry, Louisiana (30.0090°, -93.3342°) between river mile 16 and 17 (Figure 17). The demonstration area covered approximately 0.65 hectares near marsh habitat at the mouth of Kelso Bayou in 0.2 to 2 m water depths. This area is part of the Chenier Coastal Plain, which is a complex mixture of wetlands, uplands, open water, low gradient muddy shorelines or mud flats with an abundance of sediments deposited from tides and rivers (Augustinus 1989). During monitoring, the area was subjected to primarily deposited sediment inputs from Kelso Bayou, wind-driven surface wave turbulence, tidal influences (<1 m), and wakes from vessel transit in the adjacent federal navigation channel, located approximately 150 m directly east and running parallel to the demonstration area. Adjacent to the demonstration area, the authorized channel dimensions are 12 m deep by 122 m wide. The main purpose of the channel is to connect the Port of Lake Charles, Louisiana to the Gulf of Mexico. Main channel uses include the import of materials for processing at petroleum or liquefied natural gas refineries and the export of refined products. The Port of Lake Charles is the 11th largest port based on tonnage in the US with approximately 1,000 vessels per year calling at terminals located along the channel (Ausenco 2015).

Figure 17. Demonstration area near the mouth of Kelso Bayou along the Calcasieu Pass, north of Hackberry, Louisiana. The *left* inset provides a map of the US, and the *right* inset shows overview of Calcasieu Pass (Satellite photo: Google Earth).

4.1.2 Unmanned surface vehicle

The ERDC Coastal and Hydraulics Laboratory's multifunctional assessment reconnaissance vessel (MARV) is a small commercially available fishing vessel (3 m length 1 ×.2 m beam, 256 kg capacity, SURPASS® Polyethylene resin, Twin Troller X10, Angier, NC) modified to be a platform for testing and deploying a variety of environmental monitoring sensors and water collection apparatuses for aquatic applications (Figure 18). This vessel is durable and stable to allow for an easy retrofit. The plastic twin-hull designed vessel is powered by two variable speed electric motors (32 kg total thrust, 12 V) recessed into each hull, protected by metal weed guards, and a stern mounted trolling motor (20 kg thrust, 12 V) submerged about 15 cm below the water surface. The recessed hull motors are used for speed and steering (forward, reverse, 360° turns) control while the stern mounted trolling motor is locked into position and provides additional speed control only (forward, reverse). The hull design allows for a stable platform whereby water fills into the recessed areas of the hull to offset movements caused by wave action. A battery compartment near the stern carries two marine batteries (12 V lithium ion) for powering the boat motors and other electrical equipment onboard the MARV. The MARV draft is approximately 20 cm allowing it to access shallow water, and the weed guards allow for access thru submerged aquatic vegetation habitat. A remote-controlled receiver and electronic speed controllers were integrated to remotely control the recessed motors and stern trolling motor. Depending on operations, the rechargeable battery system provided sufficient power for deployment from 2–8 hr. Maneuverability of the MARV was defined by maximum speeds of approximately 4 m/s and minimum turning radius of 3 m.

Figure 18. MARV transported to demonstration area in landing craft (*top image*). MARV measuring water quality as bulk carrier ship transits north in Calcasieu Ship Channel (*bottom image*). (Photos by Justin Wilkens.)

4.1.3 Sensor integration

The MARV is a durable platform on which multiple sensors can be fitted to meet project requirements. The MARV carried an ADCP (Workhorse Rio

Grande ADCP 1200 khz, RD Instruments, Teledyne Marine, Poway, California) with a profiling range from 0.3 m to 21 m. The ADCP was used to monitor wake energy to determine the approximate time a wake entered the monitoring area and helped visualize turbidity plumes. The ADCP was mounted underwater near the center of MARV in a recessed fiberglass box fitted through an access port. A multiparameter water quality sonde (YSI 6920-V2, Yellow Springs, Ohio) used to measure conductivity, temperature, and turbidity, was attached to an electric anchor pole system (Power-Pole Micro, 12 V, JL Marine Systems, Inc., Tampa, Florida). The anchor pole system was mounted near the center of the boat on the starboard side. The manufacturer's anchor pole was replaced with two rigid electrical conduit pipes (≈ 2 m length) on which the YSI sonde was attached via hose clamps. An electronic speed controller was integrated into the anchor system which allowed the sonde to be moved up or down in the water column (0–2 m) remotely. To collect water samples (1 L) for determining TSS, a water sampler (ISCO 6712 Full-Size Portable Water Sampler, Teledyne, Poway, California) was positioned in the middle of the boat. The hose used to purge and collect the water sample was lengthened and zip tied to the end of the water quality sonde mounted on the anchor pole system. The hose was secured near the turbidity sensor to enable concurrent collection of water samples and turbidity measurements. The water sampler was controlled remotely to trigger water sample collection.

4.1.4 Monitoring

On 22 and 23 August 2018, the MARV was transported with a landing craft vessel to the demonstration area where the vessel's ramp was lowered, and the MARV was placed on the water using a winch and A-frame. The weather conditions were afternoon air temperatures near 34°C, sunny, with wind speeds <5 m/s resulting in minimal wind-driven surface wave turbulence and minimal wave-breaking. In addition to the private and commercial vessels observed in the demonstration area, the manned landing craft vessel was also used to generate data near the MARV, parallel to the ship channel. As each vessel passed, the MARV was manually controlled to different positions determined in the field within the monitoring area to collect information about the vessel wake and water quality (Figure 18). The water quality sonde was programmed to collect data every 2 sec while the ADCP data and visual observations were used to determine when a wake entered the monitoring area (Figure 19). During monitoring, real-time data were transmitted to the landing craft vessel where a computer was used to view the sonde and ADCP data. These data

were used to help position the MARV and determine when to collect water samples. Water sample collection was initiated after the wake from a passing vessel reached the shoreline and turbidity measurements were observed to be greater than background turbidity. The water sample collection was remotely triggered and verified via computer software as an incremental increase in sample number as well as an audible confirmation of water sample collection when the MARV was near the landing craft.

Figure 19. Acoustic doppler current profiler (ADCP) monitored wave energy and suspended sediments. Example ADCP profiles from two ship passing events.

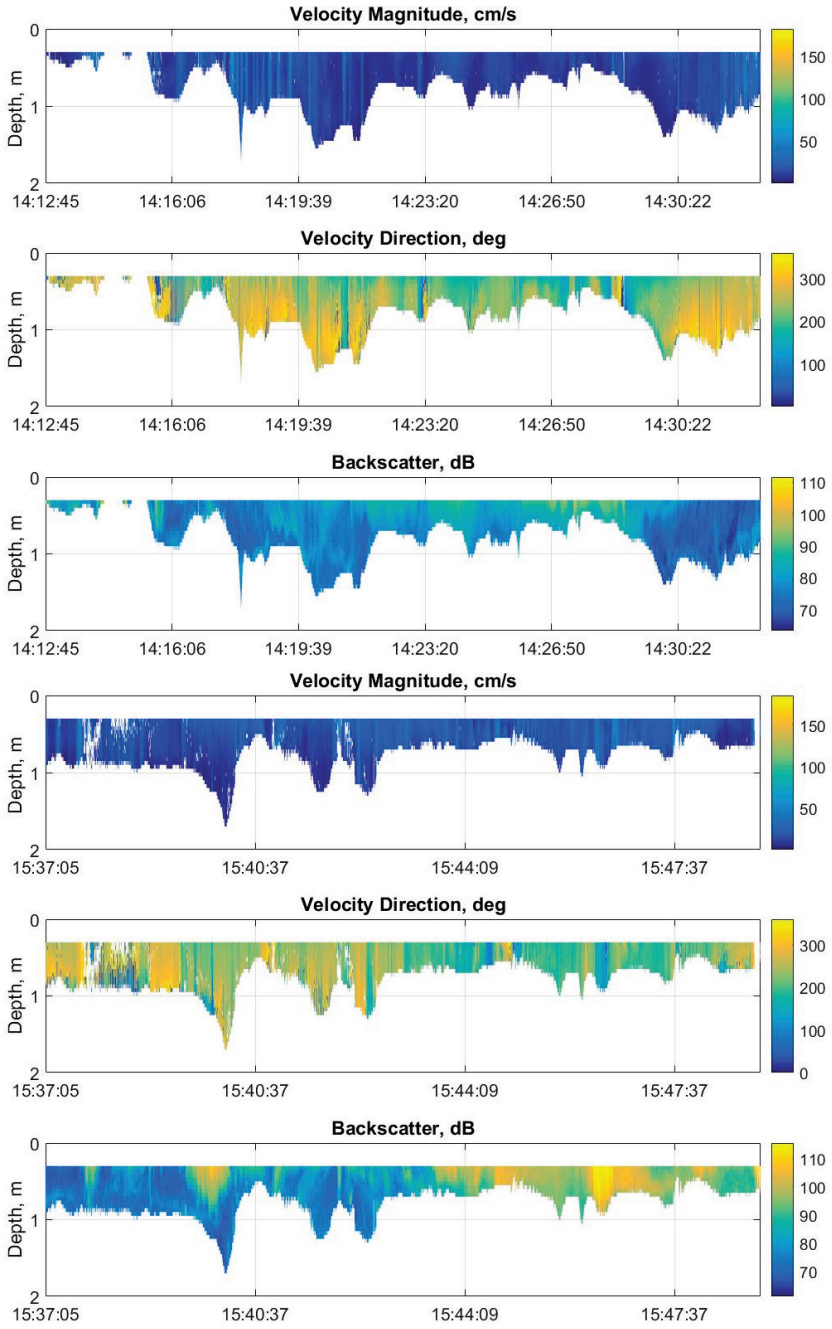

4.1.5 Sample and data processing

From each 1 L water sample, three 100 ml subsamples were collected to determine the mean TSS by gravimetric analysis (APHA 2017). To predict TSS, a TSS and NTU relationship was determined by using 5 min of NTU data centered on the time of each TSS water sample collection event. In the ship channel, a vessel wake event (north or south transit) timestamp

was recorded when the vessel was at an approximately 90-degree angle to the monitoring area. The vessels exiting from Kelso Bayou or vessels transiting north in the ship channel and then entering the Bayou from the south were timestamped when the vessel was at an approximately 180-degree angle to the monitoring area. Vessel wake event timestamps represented the start time of a wake observed to enter the monitoring area and were matched by time with water quality data to determine the effect of a vessel wake event on turbidity.

The Automatic Identification System (AIS), an automatic ship tracking system, was used to collect data on vessel type, speed, width, length, draft, and course for vessels passing by the monitoring area (Scully and McCartney 2017). For vessels not equipped with AIS tracking hardware (e.g., recreational vessels), visual observations were used to estimate vessel type, speed, width, length, draft, and course. AIS data between 01 January 2018, and 31 December 2018 were obtained to compare vessel statistics throughout the year with those data collected during the present demonstration. Using descriptive statistics, AIS data were analyzed by speed (knots), length, width, and draft (meters) for each AIS vessel type (e.g., tanker, cargo, pleasure craft, etc.).

4.2 Results and discussion

4.2.1 Vessels transiting near the monitoring area

In the shallow water monitoring area, the MARV operated in water depths ranging from 0.1 to 2 m and collected water quality data for 21 vessel wake events. Of these events, three were shipping vessels all transiting north in the channel and included the *Bulk Juliana* (bulk carrier cargo), *Brownsville* (pusher tug tanker), and the *Palmetto State* (oil/chemical tanker) (Figure 20). The remaining events, some of which were passes made by the same vessel (e.g., transited south then north past the monitoring area or vice versa), included pleasure crafts (i.e., recreational boats; n=11 events), a fast response vessel for oil spills (n=2 events), and fishing vessels (n=5 events) (Table 2). In addition to the 21 events, the landing craft vessel was used to create wakes (n=8 events) in close proximity (<30 m) to the MARV for the purpose of providing additional data (Figure 21). Except for the shipping vessels which all transited north in the channel unloaded, all other vessels transited past the monitoring area headed north or south in the channel or through Kelso Bayou. The distance between the vessels and the monitoring area was approximately

100 to 150 m for vessels passing in the channel, less than 80 m for vessels transiting through Kelso Bayou, and less than 30 m when the landing craft vessel was used. Based on AIS data, the average speed in 2018 of vessels transiting north or south in the ship channel near the monitoring area was 6.5 knots (n=2,034), with a maximum recorded speed of 32 knots (Table 3). Tanker vessels made up most vessel traffic (57.4%, mean speed 5.9 knots) followed by cargo vessels (19%, mean speed 6.5 knots), and then to a lesser frequency (<10% each) towing/tug, passenger, military, pleasure craft, fishing, pilot vessel, and sailing. Mean speed was directly related to vessel length, width, and draft and as expected the mean speed of smaller vessels (<25 m) was greatest (> 10 knots), but these vessels made up <10% of the AIS vessel traffic. The AIS data do not include small recreational vessels (e.g., recreational fishing boat, ≈6 m length, >25 knot speeds) which made up 50% of the vessels observed during this demonstration's 2-day survey.

Figure 20. Example vessels monitored during the demonstration. Top row (*left to right*): oil/chemical tanker, pusher tug tanker, bulk carrier cargo. Bottom row (*left to right*): fishing, recreational, and fast response vessels. (Photos by Justin Wilkens.)

Table 2. Vessel summary statistics based on visual observation in the field and from 2018 AIS data.

Vessel Type	Speed (knots)	Length	Width	Draft	*n*
Pleasure craft[a]	>20	≈7	≈ 6	<1	11
Landing craft vessel[b]	15	10	3	1	8
Fishing[a]	<10	≈11 (6–15)	≈ 6	≈2	5
Tanker	6 (6–7)	185 (184–185)	29 (22–36)	9	2
Fast response vessel	14	16	6	2	2
Cargo	8	190	32	7	1

[a]No AIS data available. Summary statistics are estimated based on visual observations in the field. Ranges are listed parenthetically.
[b]The landing craft vessel used to transport the MARV to the monitoring area was used to create wakes for this vessel type. Length, width, and draft reported in meters.

Figure 21. Monitoring area (*red box*); center of navigation channel (*dots*); Kelso Bayou path (*yellow line*); path traveled by ERDC landing boat (*green line*). Note: Dots represent path of AIS-equipped vessels that transit past the demonstration area in the Calcasieu River federal navigation channel between 1/1/2018 to 12/31/2018.

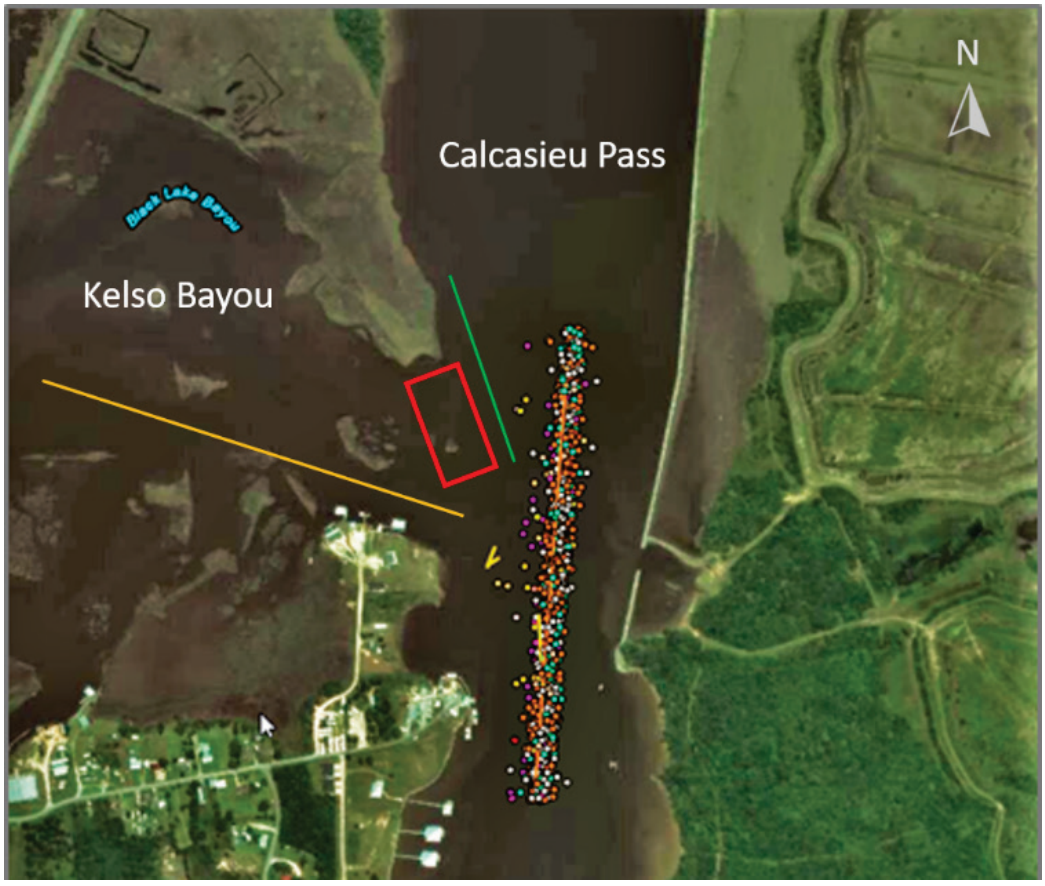

Table 3. Summary statistics of AIS 2018 vessel data (date range from 1/1/2018 to 12/31/2018) for vessels transiting the Calcasieu Ship Channel adjacent to the demonstration area (as presented visually in Figure 20).

Vessel Type	Speed (knots)	Length	Width	Draft	*n*
Tanker	6 (4–10)	197 (78–277)	34 (12–50)	10 (4–17)	1,161
Cargo	6 (4–11)	179 (30–230)	27 (9–42)	9 (3–13)	383
Other[a]	6 (4–20)	58 (13–192)	11 (2–27)	5 (1–10)	175
Towing/Tug	7 (4–12)	51 (18–206)	13 (7–28)	5 (2–9)	167
Passenger	12 (7–20)	16 (12–53)	5 (4–9)	2 (2–6)	50
Military vessel	8 (0–14)	20 (7–53)	6 (3–12)	1	40
Pleasure craft	21 (1–33)	11 (8–14)	3 (3–6)	NA	25
Fishing	6 (3–9)	24 (21–33)	7 (7–9)	2	9
Pilot vessel	12 (7–21)	220	43	7	7
Sailing	6 (5–7)	14 (13–14)	7 (4–8)	NA	4

[a]Vessel type not assigned by AIS. Range (min-max) listed parenthetically.

4.2.2 Relative influence of vessel wake of resuspension of sediment

On 22 August (Day 1), the mean (±standard deviation) turbidity level was 17 NTU (±2) and ranged from 8 to 25 NTU. During this survey period, two vessels passed the site (*Palmetto State* [oil/chemical tanker] and a pleasure craft) and had no apparent influence on sediment suspension as compared to ambient background conditions (Figure 22). On 23 August (Day 2), the mean turbidity level was relatively lower (mean 10±7 NTU) than the previous day and ranged from 3 NTU (background) to 48 NTU (maximum during wake event). In contrast to Day 1, several vessel wake events on Day 2 tracked with measurable increases in turbidity. Overall, turbidity increases following vessel wakes were relatively minor as compared to ambient background conditions (generally <40 NTU increase) and with few exceptions remained detectable for only minutes (<5 min). The largest (up to 48 NTU) and longest duration (≈10 min) of turbidity increases from background were the wakes from an apparent

cumulative effect because of multiple vessel passes. For example, the combination of the fast response vessel and bulk cargo vessel passing the demonstration area within minutes of each other and quick successive passes (n = 5 events within 10 min) by the ERDC landing craft vessel. The lack of an apparent relation between vessel wake events and increased turbidity on Day 1 is likely due to a higher mean background turbidity level on this day that partly masked the minor increases in turbidity following a vessel wake event. Additionally, unlike Day 2 where successive vessel passes caused visible turbidity, there were no successive vessel passes on Day 1. In the demonstration area, the threshold between background turbidity and turbidity generated by a vessel wake event most likely depends on factors such as increases in turbidity originating from Kelso Bayou, wind velocity, sailing speed of vessels, vessel type and distance to shoreline, interval between successive passes, bathymetry, and finally, the position of the MARV during data collection.

Figure 22. Day 1 turbidity (NTU) measured by the MARV in a shallow-water marsh in relation to passing vessel wakes for vessels listed in Table 2.

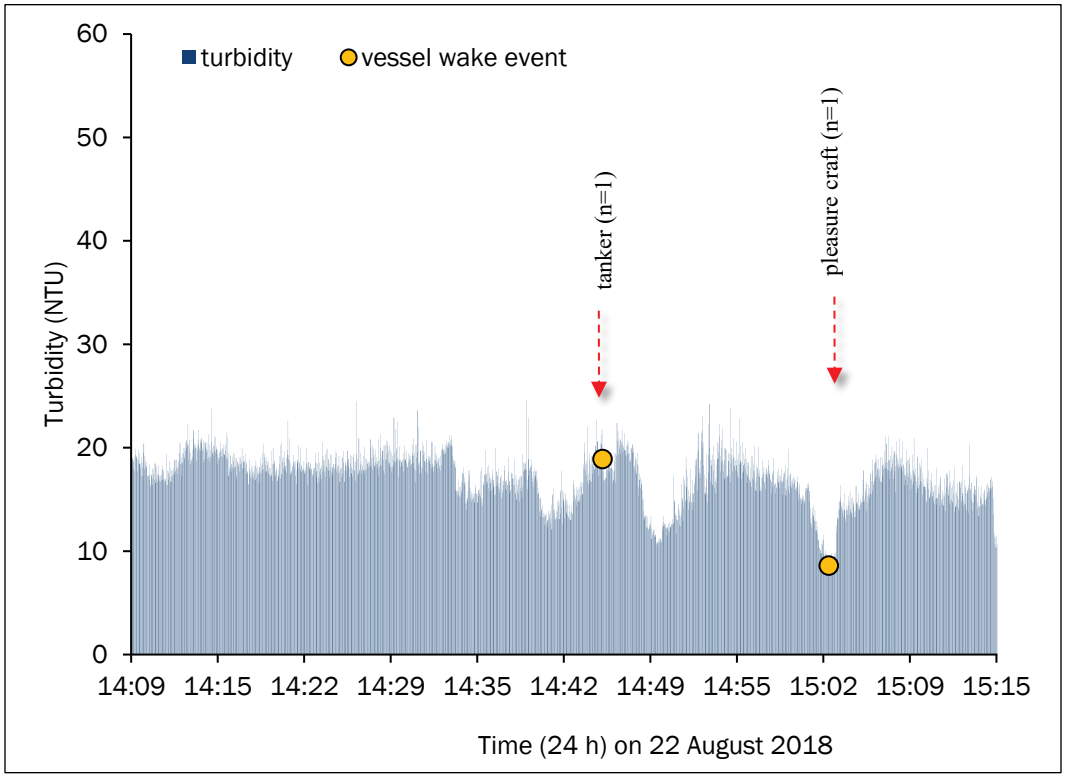

Figure 23. Day 2 turbidity (NTU) measured by the MARV in a shallow water marsh in relation to passing vessel wakes for vessels listed in Table 2.

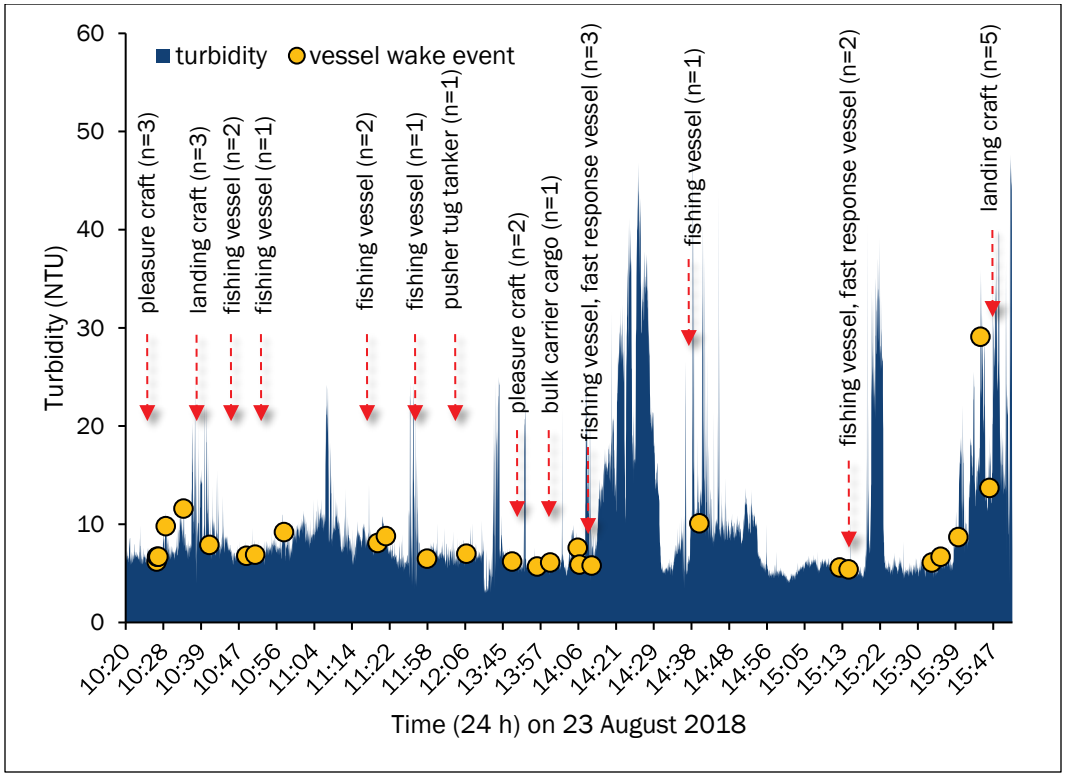

Linear regression analysis of TSS concentrations as a function of turbidity resulted in a relatively weak correlation coefficient between TSS and turbidity (n=40, y=2.379×-20818, R=0.69). The regression equation predicts the TSS of the highest turbidity observed in this demonstration (48 NTU) to be approximately 112 mg/L. The TSS-NTU relationship indicates the challenges in obtaining paired TSS-NTU field samples representative of the demonstration area from the MARV with the current water collection apparatus. The anchor pole system successfully moved the sonde and water collection tube through the water column, but it was challenging to determine where in the water column the sampler was which led to unforeseen operator errors (e.g., sampling bottom sediments). Additional samples and modifications to the anchor pole systems to help the operator view sampling depth would improve the relationship. Overall, within the constraints of this demonstration and in context to the natural background conditions, these data indicate the potential contribution of a vessels wake to the resuspension of sediment in shallow water habitat, particularly near the shoreline-water interface, and highlights the cumulative effects of quick successive passes (i.e., increased vessel traffic) resulting in increased turbidity.

4.2.3 Use of a USV for dredge plume monitoring in shallow water

The MARV platform provided an opportunity to capture the spatial and temporal monitoring requirements using a range of environmental sensors. The MARV is more adaptable and flexible for working in shallow water areas compared with manned vessels or buoy-based monitoring systems and deployment is highly repeatable to allow for high spatial and temporal resolution data. The cost for acquiring field data using the MARV platform includes the initial platform investment and retrofit with environmental sensors, processing software, data storage, and fieldwork expenses. In terms of using the MARV for monitoring dredging operations, it will likely be most competitive when the acquisition of data in small areas (< 10 ha) such as sensitive shallow water habitats are required to monitor the potentially rapid changes of water quality due to dredging activities. At the current time, a review on the use of UAS for environmental monitoring suggests that UAS are most effective over areas 10–20 ha in size, while exceedingly larger areas result in increased costs for data acquisition and postprocessing and can negatively affect the economic benefits of using UAS as compared to a manned aircraft (Manfreda et al. 2018). This is likely also a good rule of thumb for USV data acquisition. While the MARV and other USVs cannot compete with the spatial coverage of manned vessels, they can provide potentially high spatial and temporal resolutions in shallow areas inaccessible to manned vessels. Based on the performance of MARV, this platform and other comparable platforms can provide sufficient capabilities to perform water quality monitoring in shallow water sensitive habitats.

4.3 Summary of estimating turbidity and suspended sediment concentrations using an unmanned surface vehicle

The shallow marsh habitat adjacent to the Calcasieu Ship Channel in southern Louisiana provided an opportunity to evaluate the capabilities of a USV for monitoring suspended sediments in the water column. The goal of this demonstration was to improve knowledge of the efficacies and limitations of these platforms in sensitive shallow water habitats, as possible benefits on USVs are realized for water quality monitoring. A USV was successfully modified with complementing sensing and sampling platforms including a water quality sonde, turbidity sensor, water sampler, and ADCP. During the survey, the site was traversed by a variety of vessels of different types and sizes (n=21), providing opportunities to measure the effects of vessel wake events on the suspension of sediments in the marsh.

Turbidity increases following vessel wake events were generally minor, with a maximum increase of less than 40 NTU compared to ambient background conditions. An added benefit of the USV was the cocollected ADCP and in situ water sampling to contextualize and validate turbidity observations in real time. Data from this field demonstration indicates USVs provide a robust and flexible approach to monitoring suspended sediments in shallow water areas. Although USVs cannot compete with the spatial coverage extent of manned vessels, they can provide potentially high spatial and temporal resolution in shallow water areas inaccessible by manned vessels. Based on the performance of the USV used in this demonstration, it provided capabilities to perform water quality monitoring in shallow water habitats that would be beneficial for dredge sediment plume monitoring. Specifically, the spatial and temporal resolution of data collected by the USV could provide sufficient quantity and quality to facilitate communication with regulatory agencies and stakeholders to inform dredge operation and management decisions.

5 Summary and Recommendations

In summary, the use of unmanned technology, such as UAS, weather balloon-mounted camera imagery, and USV, has the potential to provide benefits in monitoring turbidity, especially in dredging operations. This study demonstrated that unmanned technology could produce easily interpretable aerial imagery and estimates of turbidity that can be compared to in-situ measurements to provide evidence-based information. Considerations such as monitoring context, time interval, mobility, scale, accuracy, and type of dissemination product should be considered when selecting the most appropriate unmanned technologies for water quality monitoring. Despite these considerations, the use of unmanned surveys could substantially improve the USACE's ability to estimate the potential impacts of dredging operations, particularly near sensitive habitats, and ultimately improve decision-making in dredging operations.

References

APHA (American Public Health Association). 2017. *Standard methods for the examination of water and wastewater*, 23rd ed. Baltimore, MD: Port City Press.

Augustinus, P. G. E. F. 1989. "Cheniers and Chenier Plains: A General Introduction." *Marine Geology* 90, no. 4: 219–29. https://doi.org/10.1016/0025-3227(89)90126-6.

Ausenco. 2015. "Calcasieu Ship Channel Traffic Study (Report 100218-01-RPT-0001)." Retrieved from http://www.portlc.com/calcasieu-ship-channel/channel-traffic-study/.

Binding, C. E., D. G. Bowers, and E. G. Mitchelson-Jacob. 2005. "Estimating Suspended Sediment Concentrations from Ocean Colour Measurements in Moderately Turbid Waters; the Impact of Variable Particle Scattering Properties." *Remote Sensing of Environment* 94, no. 3: 373–83. https://doi.org/10.1016/j.rse.2004.11.002.

Clarke, D. G., and D. H. Wilber. 2008. "Compliance Monitoring of Dredging-Induced Turbidity: Defective Designs and Potential Solutions." In *Proceedings of the Western Dredging Association 28th Technical Conference*. WEDA, St. Louis, USA.

Congedo, L. 2016. Semi-automatic classification plugin documentation. Release 5.0.2.1, 201 pp. https://fromgistors.blogspot.com/p/semi-automatic-classification-plugin.html (Retrieved 3 January 2017).Curran, P. J., and E. M. M. Novo. 1988. "The Relationship between Suspended Sediment Concentration and Remotely Sensed Spectral Radiance: A Review." *Journal of Coastal Research* 4: 351–68.

Dekker, A. G., R. J. Vos, and S. W. Peters. 2001. "Comparison of Remote Sensing Data, Model Results and in Situ Data for Total Suspended Matter (TSM) in the Southern Frisian Lakes." *The Science of the Total Environment* 268, no. 1–3: 197–214. https://www.ncbi.nlm.nih.gov/pubmed/11315742.

Dörnhöfer, K., and N. Oppelt. 2016. "Remote Sensing for Lake Research and Monitoring-Recent Advances." *Ecological Indicators* 64: 105–22.

Doxaran, D., J-M Froidefond, and P. Castaing. 2002. "A Reflectance Band Ratio Used to Estimate Suspended Matter Concentrations in Sediment-Dominated Coastal Waters." *International Journal of Remote Sensing* 23(23): 5079–85. https://doi.org/10.1080/0143116021000009912.

Dunbabin, M., and A. Grinham. 2010. "Experimental Evaluation of an Autonomous Surface Vehicle for Water Quality and Greenhouse Gas Emission Monitoring." In *2010 IEEE International Conference on Robotics and Automation (ICRA)*, 5268–74. IEEE.

Haque, A., and K. K. Adhikary. 2016. Estimation of suspended sediment concentration of water bodies using low cost portable digital camera. *Proceedings of 3rd International Conference on Advances in Civil Engineering*, Chittagong, Bangladesh, December 21–23. https://www.cuet.ac.bd/icace/papers/water/248.pdf.

Jones, Ross, Rebecca Fisher, and Pia Bessell-Browne. 2019. "Sediment Deposition and Coral Smothering." *PloS One* 14(6): e0216248. https://doi.org/10.1371/journal.pone.0216248.

Küng, O., C. Strecha, A. Beyeler, J-C Zufferey, D. Floreano, P. Fua, and F. Gervaix. 2011. "The Accuracy of Automatic Photogrammetric Techniques on Uultrla-Lltraight UAV Imagery." In *UAV-g 2011-Unmanned Aerial Vehicle in Geomatics*.

Kutser, T., L. Metsamaa, E. Vahtmae, and R. Aps. 2007. "Operative Monitoring of the Extent of Dredging Plumes in Coastal Ecosystems Using MODIS Satellite Imagery." In *SI 50 (Proceedings of the 9th International Coastal Symposium*, 180–84. Gold Coast, Australia.

Liu, Yansui, Md Anisul Islam, and Jay Gao. 2003. "Quantification of Shallow Water Quality Parameters by Means of Remote Sensing." *Progress in Physical Geography* 27(1): 24–43. https://doi.org/10.1191/0309133303pp357ra.

Liu, Zhixiang, Youmin Zhang, Xiang Yu, and Chi Yuan. 2016. "Unmanned Surface Vehicles: An Overview of Developments and Challenges." *Annual Reviews in Control* 41: 71–93. https://doi.org/10.1016/j.arcontrol.2016.04.018.

Manfreda, S. McCabe, M. W., Miller, P. E., Lucas, R., Madrigal, V. P., Mallinis, G., Dor, E. B., Helman, D., Estes, L., Ciraolo, G., Mullerova, J., Tauro, F., De Lima, M. I., De Lima, J. L. M. P., Maltese, A., Frances, F., Caylor, K., Kohv, M., Perks, M., Ruiz-Perez, G., Su, Z., Vico, G., and Toth, B. 2018. "On the use of unmanned aerial systems for environmental monitoring." *Remote sensing* 10:641.Matthews, Mark William. 2011. "A Current Review of Empirical Procedures of Remote Sensing in Inland and Near-Coastal Transitional Waters." *International Journal of Remote Sensing* 32(21): 6855–99. https://doi.org/10.1080/01431161.2010.512947.

Mogstad, Aksel Alstad, Geir Johnsen, and Martin Ludvigsen. 2019. "Shallow-Water Habitat Mapping Using Underwater Hyperspectral Imaging from an Unmanned Surface Vehicle: A Pilot Study." *Remote Sensing* 11(6): 685. https://doi.org/10.3390/rs11060685.

Puckette, T. P. 1998. *Evaluation of Dredged Material Plumes Physical Monitoring Techniques*. ERDC TN-DOER-E5. Vicksburg MS: US Army Engineer Research and Development Center. https://el.erdc.usace.army.mil/.Python Software Foundation (PSF). 2018. Python version 2.7. Available online: https://www.python.org (accessed on 29 March 2018).

Reine, K. J., D. D. Dickerson, and D. G. Clarke. 1998. *Environmental Windows Associated with Dredging Operations*. ERDC TN DOER-E2. Vicksburg, MS: US Army Engineer Research and Development Center. http://el.erdc.usace.army.mil/

Roze, A., J. C. Zufferey, A. Beyeler, and A. McClellan. 2014. eBee RTK accuracy assessment (white paper). https://www.sensefly.com/fileadmin/user_upload/sensefly/documents/eBee-RTK-AccuracyAssessment.pdf. (Retrieved on 3 January 2017).

Scully, B. M., and A. C. McCartney. 2017. *Use of AIS and AISAP for Analysis of Vessel Wakes in Charleston Harbor: A Case Study*. ERDC-CHL CHETN-IX-46. US Army Engineer Research and Development Center. Vicksburg, MS. http://dx.doi.org/10.21079/11681/22908.

Shi, Wei, and Menghua Wang. 2009. "Satellite Observations of Flood-Driven Mississippi River Plume in the Spring of 2008." *Geophysical Research Letters* 36(7). https://doi.org/10.1029/2009gl037210.

Steimle, E. T., and M. L. Hall. 2006. "Unmanned surface vehicles as environmental monitoring and assessment tools." *OCEANS 2006:*1–5.

Suedel, Burton C., Jongbum Kim, Douglas G. Clarke, and Igor Linkov. 2008. "A Risk-Informed Decision Framework for Setting Environmental Windows for Dredging Projects." *The Science of the Total Environment* 403(1–3): 1–11. https://doi.org/10.1016/j.scitotenv.2008.04.055.

US Department of the Army. (2018). Aviation Flight Regulations*: Army regulation 95–1*. https://armypubs.army.mil/ProductMaps/PubForm/Details.aspx?PUB_ID=1003624

Vogt, Michael C., and Mark E. Vogt. 2016. "Research Article: Near-Remote Sensing of Water Turbidity Using Small Unmanned Aircraft Systems." *Environmental Practice: Journal of the National Association of Environmental Professionals* 18(1): 18–31. https://doi.org/10.1017/s1466046615000459.

Walker, N. D., and A. B. Hammack. 2000. "Impacts of Winter Storms on Circulation and Sediment Transport: Atchafalaya-Vermilion Bay Region." *Journal of Coastal Research*, 996–1010.

Watts, Adam C., John H. Perry, Scot E. Smith, Matthew A. Burgess, Benjamin E. Wilkinson, Zoltan Szantoi, Peter G. Ifju, and H. Franklin Percival. 2010. "Small Unmanned Aircraft Systems for Low-Altitude Aerial Surveys." *The Journal of Wildlife Management* 74(7): 1614–19. https://doi.org/10.2193/2009-425.

Wells, J. T., and G. P. Kemp. 1981. "Atchafalaya Mud Stream and Recent Mudflat Progradation: Louisiana Chenier Plain." *Transactions-Gulf Coast Association of Geological Societies*, 409–16.

Wilber, Dara H., and Douglas G. Clarke. 2001. "Biological Effects of Suspended Sediments: A Review of Suspended Sediment Impacts on Fish and Shellfish with Relation to Dredging Activities in Estuaries." *North American Journal of Fisheries Management* 21(4): 855–75. https://doi.org/10.1577/1548-8675(2001)021<0855:beossa>2.0.co;2.

Zeng, Chuiqing, Murray Richardson, and Douglas J. King. 2017. "The Impacts of Environmental Variables on Water Reflectance Measured Using a Lightweight Unmanned Aerial Vehicle (UAV)-Based Spectrometer System." *ISPRS Journal of Photogrammetry and Remote Sensing: Official Publication of the International Society for Photogrammetry and Remote Sensing (ISPRS)* 130: 217–30. https://doi.org/10.1016/j.isprsjprs.2017.06.004.

REPORT DOCUMENTATION PAGE

1. REPORT DATE	2. REPORT TYPE	3. DATES COVERED	
		START DATE	END DATE
August 2023	Final report	FY	FY

4. TITLE AND SUBTITLE

Improving Spatial and Temporal Monitoring of Dredging Operations Incorporating Unmanned Technologies

5a. CONTRACT NUMBER	5b. GRANT NUMBER	5c. PROGRAM ELEMENT
5d. PROJECT NUMBER	**5e. TASK NUMBER**	**5f. WORK UNIT NUMBER**

6. AUTHOR(S)

Justin L. Wilkens, Andrew D. McQueen, and Burton C. Suedel

7. PERFORMING ORGANIZATION NAME(S) AND ADDRESS(ES)

US Army Engineer Research and Development Center
Environmental Laboratory
3909 Halls Ferry Rd
Vicksburg, MS 39180-6199

8. PERFORMING ORGANIZATION REPORT NUMBER

ERDC/EL TR-23-4

9. SPONSORING/MONITORING AGENCY NAME(S) AND ADDRESS(ES)	10. SPONSOR/MONITOR'S ACRONYM(S)	11. SPONSOR/MONITOR'S REPORT NUMBER(S)
US Army Corps of Engineers Washington, DC 20314-1000		

12. DISTRIBUTION/AVAILABILITY STATEMENT

DISTRIBUTION STATEMENT A. Approved for public release. Distribution is unlimited.

13. SUPPLEMENTARY NOTES

Funding Element U451408, Funding account U4349741, AMSCO Code 089500, "Improving Spatial Monitoring of Dredging Operations with Unmanned Systems"

14. ABSTRACT

The US Army Corps of Engineers (USACE) is responsible for maintaining safe and navigable waterways through the periodic dredging of shoaled sediment from federal navigation channels. While dredging, a portion of the bottom sediments become resuspended creating a sediment plume near the dredging operation. Suspension of sediments during dredging and dredged sediment disposal operations continues to be a primary concern of regulatory agencies charged with the protection of environmental resources. Consequently, almost all dredging projects incorporate some level of regulatory compliance monitoring dedicated to measuring sediment resuspension. For numerous reasons the conventional approach using manned surface vessels to perform compliance monitoring is frequently ineffective in both adaptively managing dredging projects and ensuring true environmental protection. Advancements in unmanned platforms and payload technologies offer new and potentially more robust alternatives to conventional platforms. In this study, the use of unmanned aerial system (UAS) and weather balloon mounted camera imagery was demonstrated, and the use of an unmanned surface vessel (USV) to monitor turbidity in navigation channels and near a dredging operation. The imagery from the UAS and weather balloon were compared to in-situ turbidity measurements in a turbid distributary channel and near a dredging operation, while the USV was used to learn more about in-situ turbidity associated with passing vessels in a navigation channel. The results of the demonstrations show the unmanned technology bundled with off-the-shelf payloads can help to produce evidence-based information through easily interpreted aerial imagery and in situ measurements which can help to inform and manage water quality in areas where sediment plumes are an environmental concern.

15. SUBJECT TERMS

Dredging—Monitoring
Suspended sediments—Monitoring
Turbidity—Monitoring
Remote sensing
Drone aircraft
Automated vehicles--Boats

16. SECURITY CLASSIFICATION OF:			17. LIMITATION OF ABSTRACT	18. NUMBER OF PAGES
a. REPORT	b. ABSTRACT	C. THIS PAGE		
Unclassified	Unclassified	Unclassified	SAR	62

19a. NAME OF RESPONSIBLE PERSON	19b. TELEPHONE NUMBER (include area code)